Impacts of Temperature, CO$_2$, and Salinity on Phytoplankton Community Composition in the Western Arctic Ocean

Koji Sugie[1]*, Amane Fujiwara[1], Shigeto Nishino[1], Sohiko Kameyama[2] and Naomi Harada[1]

[1] Research Institute for Global Change, Japan Agency for Marine-Earth Science and Technology, Yokosuka, Japan, [2] Faculty of Environmental Earth Science, Hokkaido University, Sapporo, Japan

The Arctic Ocean has been experiencing rapid warming, which accelerates sea ice melt. Further, the increasing area and duration of sea ice-free conditions enhance ocean uptake of CO$_2$. We conducted two shipboard experiments in September 2015 and 2016 to examine the effects of temperature, CO$_2$, and salinity on phytoplankton dynamics to better understand the impacts of rapid environmental changes on the Arctic ecosystem. Two temperature conditions (control: <3 and 5°C above the control), two CO$_2$ levels (control: ~300 and 300/450 µatm above the control; i.e., 600/750 µatm), and two salinity conditions (control: 29 in 2015 and 27 in 2016, and 1.4 below the control) conditions were fully factorially manipulated in eight treatments. Higher temperatures enhanced almost all phytoplankton traits in both experiments in terms of chl-*a*, accessory pigments and diatom biomass. The diatom diversity index decreased due to the replacement of chain-forming *Thalassiosira* spp. by solitary *Cylindrotheca closterium* or *Pseudo-nitzschia* spp. under higher temperature and lower salinity in combination. Higher CO$_2$ levels significantly increased the growth of small-sized phytoplankton (<10 µm) in both years. Decreased salinity had marginal effects but significantly increased the growth of small-sized phytoplankton under higher CO$_2$ levels in terms of chl-*a* in 2015. Our results suggest that the smaller phytoplankton tend to dominate in the shelf edge region of the Chukchi Sea in the western Arctic Ocean under multiple environmental perturbations.

Keywords: the Arctic Ocean, global warming, ocean acidification, sea ice melt, phytoplankton, ecosystem structure

INTRODUCTION

The ocean mitigates global climate change by absorbing heat and atmospheric CO$_2$, resulting in warming and acidification of the sea surface. Changes are particularly prominent in the Arctic and are referred to as Arctic amplification (Serreze and Barry, 2011; AMAP, 2013). Warming in the Arctic over the last few decades is actually more than twice that measured in the lower latitudes, and further warming in the Arctic is expected if the current growth in greenhouse

gas (e.g., carbon dioxide: CO_2) emissions continues (Overland et al., 2014). Approximately one-third of the anthropogenic CO_2 released into the atmosphere dissolves in seawater causing ocean acidification (Doney et al., 2009). The impact of CO_2-induced acidification is most severe in the Arctic Ocean, especially in terms of the saturation state of calcium carbonate (AMAP, 2013; Yamamoto-Kawai et al., 2016). Furthermore, freshwater input to the Arctic Ocean has increased because of the increase in sea ice melt and meteoric water as a result of warming (Comiso et al., 2008; Koenigk et al., 2013). Recent persistence of strong anticyclonic circulations has led to the accumulation of freshwater in the oceanic gyres, such as the Beaufort Gyre, resulting in decreased salinity (Proshutinsky et al., 2015). Organisms in the Arctic Ocean must cope with multiple environmental perturbations. However, the effects of these environmental changes on the ecosystem processes in the Arctic Ocean are poorly understood.

Marine phytoplankton, forming the base of the marine ecosystem, have already been affected by changes in the Arctic. A shorter sea ice season as a result of earlier sea ice retreat and later freeze-up results in increases in the exposure of the sea surface to sunlight and wind stress, which has altered the productivity and phenology of phytoplankton blooms (Arrigo and van Dijken, 2011; Ardyna et al., 2014; Nishino et al., 2015; Fujiwara et al., 2018). In the Canada Basin of the western Arctic Ocean, the composition of pico-sized ($<2\ \mu m$ in diameter) phytoplankton tended to increase with time, probably due to low nutrient availability in strongly stratified surface waters under warmer and fresher conditions (Li et al., 2009; Ardyna et al., 2017). However, it is often difficult to discriminate between the effects of different environmental factors on phytoplankton dynamics from *in situ* monitoring data because of the relatively low frequency of observations and the complexity of the ocean. To better understand the impact of each environmental perturbation, it is indispensable to conduct incubation/culture experiments using the natural plankton communities or the unialgal culture of key phytoplankton species (Sugie and Yoshimura, 2013, 2016; Boyd et al., 2016; Schulz et al., 2017).

The effects of environmental perturbations such as changes in temperature and CO_2 levels on marine phytoplankton are mostly examined through manipulation experiments. Although numerous studies from the previous decades have reported temperature and/or CO_2 manipulation experiments (Yoshimura et al., 2014; Schulz et al., 2017 and references therein), few have focused on the Arctic Ocean. A few experiments have been conducted in the eastern Arctic Ocean, but the results were inconsistent with one another (Schulz et al., 2013; Holding et al., 2015; Hoppe et al., 2017; Wolf et al., 2018). For example, Holding et al. (2015) reported an enhancement of primary productivity under increased CO_2 levels, whereas Hoppe et al. (2017) did not. In terms of community composition, eukaryotic picophytoplankton (PicoE) tended to dominate under the higher CO_2 levels (Schulz et al., 2013). Species shifts occurred between different diatom species that were functionally similar (Hoppe et al., 2017); the lack of change in species composition was probably caused by intraspecific variability in the responses of dominant diatom species to CO_2 variations (Wolf et al., 2018).

Although multiple environmental factors change simultaneously, previous studies rarely examined the combined effects of more than two perturbations on plankton communities (Boyd et al., 2016). Additional experiments are needed to clarify the impact of multiple environmental perturbations on the response of phytoplankton communities and hence on the dynamics of the Arctic ecosystem. Previous manipulation experiments were conducted in the eastern Arctic Ocean, where the ecosystem structure is substantially different from that in the western Arctic (Hunt et al., 2013; Grebmeier et al., 2015).

From the Chukchi Sea and Beaufort Sea to the Canada Basin of the western Arctic, primary production and the standing stock of phytoplankton decrease with latitude (Coupel et al., 2015; Nishino et al., 2016). Biological carbon sequestration to deeper layers can occur only in the Canada Basin, although phytoplankton production is low as a result of low nitrate availability (Watanabe et al., 2014; Ardyna et al., 2017). In the Arctic oligotrophic oceanic region, lateral transport of resuspended particulate organic matter (S-POM) from the bottom of the continental shelf plays a key role in the biological carbon pump (Watanabe et al., 2014; Harada, 2016). As a result, the quality and quantity of particulate organic matter produced in the water column on the continental shelf are some of the most important factors that determine the transfer efficiency of organic carbon to the deeper Canada Basin. To the best of our knowledge, very limited information is available concerning the impact of multiple environmental perturbations on the phytoplankton community structure in the western Arctic Ocean.

In the present study, we investigated the interactive effects of changes in temperature, CO_2 and salinity on phytoplankton communities in the western Arctic Ocean in two consecutive years. We focused on the response of phytoplankton size and community composition to multiple environmental perturbations because the size of organisms is a prime trait affecting all aspects of ecosystem dynamics, such as trophic interaction and biogeochemical cycling of carbon and nutrients (Thingstad et al., 2005; Edwards et al., 2013; Marañón, 2015). For example, the food chain that dominates smaller primary producers such as pico-sized phytoplankton leads to an increase in the number of trophic levels in a local ecosystem compared with that dominate larger ones such as diatoms. Because a large part of energy (80–90%) loss through respiration occurs during transfer between preys and predators, the number of trophic levels, i.e., the size of primary producers is primarily important to understand the production of higher trophic levels (Lalli and Parsons, 1997).

MATERIALS AND METHODS

Sampling and Experimental Setup

Manipulation experiments were conducted in the northern Chukchi Sea in the western Arctic Ocean on 14 September 2015 at 71.7°N, 155.2°W, and 15 September 2016 at 73.3°N, 160.8°W aboard *R/V* Mirai (Japan Agency for Marine-Earth Science and Technology) during the MR15-03 and MR16-06 cruises, respectively (hereafter referred to as MR15-exp. and

MR16-exp.; **Figure 1**). The stations of MR15 and MR16 were located near the Barrow and Hanna Canyons, respectively, which are the source areas of the S-POM in the Canada Basin (Watanabe et al., 2014). Two temperature regimes, two CO_2 levels and two salinity conditions were manipulated using a fully factorial design (i.e., 2^3) in eight treatments to understand the impacts of single and multiple environmental perturbations responsible for the change in community structure of phytoplankton (**Table 1**). The temperature regimes were the lower temperature (LT representing *in situ* temperature) and the higher temperature (HT) regimes, and the HT was approximately 5°C higher than the LT. The CO_2 levels were the control level (*in situ*: ~300 μatm) and the higher CO_2 (HC) level, which in MR15-exp., was 300 μatm higher partial pressure of CO_2 (pCO_2) than that of the controls, and in the MR16-exp., was 450 μatm higher pCO_2 than that of the controls. The salinity conditions were the control (*in situ*: 29.2 in the MR15-exp. and 27.3 in the MR16-exp.) and the LS condition, which was 1.4 lower than that of the control (**Table 1**). The values adopted in the high temperature, high CO_2, and low salinity conditions were chosen to approximate future conditions in the Arctic Ocean as simulated under representative concentration pathways (RCP) 4.5 and 8.5 scenarios expected in the future Arctic Ocean (AMAP, 2013; Koenigk et al., 2013; Overland et al., 2014). For example, the predictions of temperature rise at the end of this century ranged about 3°C in surface mixed layer (~100 m) or 6–13°C in the surface air under the RCP8.5 scenario (Overland et al., 2014). Environmental conditions at the surface of the Chukchi Sea are highly dynamic in space and time ranging between 0 and 8°C for temperature, between <250 and ~350 μatm pCO_2 and between 24 and 32 for salinity (Nishino et al., 2016; Yamamoto-Kawai et al., 2016; Yasunaka et al., 2018). Extremely high CO_2 levels ranging from 700 to >1000 μatm have been observed just below the surface mixed layer from September to October (Yamamoto-Kawai et al., 2016). This indicates that the results from this study

would contribute to a better understanding of the response of the phytoplankton community to the dynamic environmental changes that are currently taking place in the Arctic Ocean.

For incubation experiments, seawater samples were collected at depth of 10 m (MR15-exp.) and 15 m (MR16-exp.) using acid-washed, Teflon-coated 12 L Niskin-X sampling bottles (General Oceanics Inc., Miami, FL, United States) attached to a conductivity temperature depth profiler with a carousel multiple sampling (CTD-CMS) system. At these depths, photosynthetically active radiation (PAR) levels were approximately 50% of surface PAR levels (Fujiwara, A., unpublished data obtained using PRR800 in 2015 or C-OPS in 2016; Biospherical Instruments Inc., San Diego, CA, United States, and available at http://www.godac.jamstec.go.jp/darwin/cruise/mirai/mr15-03_leg1/e and http://www.godac.jamstec.go.jp/darwin/cruise/mirai/mr16-06/e). Seawater was filtered through an acid-cleaned 200 μm Teflon mesh attached to silicon tubes to eliminate large zooplankton. In the MR15-exp., pre-screened seawater was poured into four acid-washed 50 L polypropylene carboys, followed by adding a small amount of filtered seawater saturated with CO_2 at 1 atm to carboys No. 1 and 2 for the HC series (Gattuso et al., 2011). For the LS series, 2.5 L of Milli-Q water (18.2 MΩcm; Merck KGaA, Darmstadt, Germany) was added to carboys No. 2 and 4. For the control salinity series, 2.5 L of filtered seawater, made using acid-washed 0.2 μm pore-sized capsule filters (Pall Corp., New York, NY, United States), was added to carboys No. 1 and 3. After that, nutrients (NO_3: 7 μmol L^{-1}, PO_4: 0.5 μmol L^{-1}, and $Si(OH)_4$: 5 μmol L^{-1}, in final concentrations) were added to all carboys prior to homogenizing the seawater. Nutrients were added to mask the effects of nutrient limitation and to mimic wind-induced nutrient upwelling, which is frequently observed in autumn along the shelf edge in the Chukchi Sea and Canada Basin, where sea ice has retreated during the summer and autumn (Nishino et al., 2015; Ardyna et al., 2017; Fujiwara et al., 2018). Note that although the added nutrient stock solutions were prepared using Milli-Q water, the amount of the additions was very small compared to that of the incubation bag (<0.1% in v/v), and the change in salinity should be consistent in all bags. Seawater was dispensed into four 10 L polyethylene incubation bags from each carboy; i.e., 16 bags, eight bags were used for the LT series (LT, LTHC, LTLS, LTLSHC), and another eight bags were used for the HT series (HT, HTHC, HTLS, HTLSHC), providing duplicates for each treatment. Finally, a small amount of 0.1 mol L^{-1} NaOH (Suprapur, Merck KGaA, Darmstadt, Germany) was added to the incubation bags of the HT series to offset the temperature-driven increase in pCO_2. In the MR16-exp., the experimental procedures were slightly modified using a seawater distribution system. Seawater was poured from six Niskin-X sampling bottles into the bottom of a custom-made 4 L polypropylene bottles, which had six inlets in the bottom and six outlets in the upper part (**Supplementary Figure S1A**). Seawater from the bottle was distributed into twelve 10 L polyethylene incubation bags using silicon tubing attached to an acid-cleaned 200 μm Teflon mesh to obtain homogenized samples (**Supplementary Figure S1B**). We prepared two sets of seawater distribution systems and made 24 incubation bags,

FIGURE 1 | Sampling locations in the western Arctic Ocean with names of the incubation experiments.
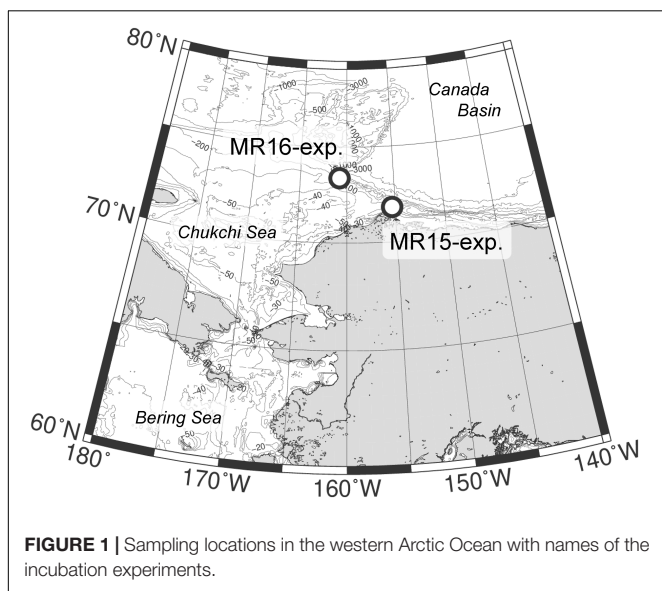
TABLE 1 | Results of carbonate chemistry during the two experiments. LT and HT represent low- and high-temperature treatment, respectively.

	Day 2 (HT) or Day 3 (LT)				Day 6 (MR15-exp. HT), Day 7 (MR16-exp. HT) or Day 8 (LT)			
	DIC (μmol kg^{-1})	TA (μmol kg^{-1})	pCO_2 (μatm)	pH (Total scale)	DIC (μmol kg-1)	TA (μmol kg^{-1})	pCO_2 (μatm)	pH (Total scale)
MR15-xp								
LT	1944 ± 0.6	2082 ± 2.6	289 ± 6.1	8.14 ± 0.01	1938 ± 0.7	2086 ± 0.4	269 ± 1.9	8.17 ± 0.00
LTHC	2028 ± 0.1	2079 ± 1.5	588 ± 7.9	7.86 ± 0.01	2018 ± 1.1	2084 ± 0.3	516 ± 6.4	7.91 ± 0.01
LTLS	1876 ± 9.5	1997 ± 7.9	292 ± 5.6	8.13 ± 0.01	1866 ± 7.9	1999 ± 6.8	266 ± 3.6	8.16 ± 0.01
LTHCLS	1936 ± 0.1	1979 ± 1.6	580 ± 8.1	7.85 ± 0.01	1927 ± 0.5	1983 ± 0.5	521 ± 0.1	7.89 ± 0.00
HT	1945 ± 0.8	2107 ± 0.1	310 ± 1.5	8.13 ± 0.00	1926 ± 0.6	2111 ± 3.2	265 ± 5.8	8.14 ± 0.01
HTHC	2029 ± 0.7	2090 ± 1.2	669 ± 2.3	7.82 ± 0.00	2003 ± 0.9	2093 ± 0.3	521 ± 5.0	7.91 ± 0.05
HTLS	1838 ± 4.4	1982 ± 5.5	299 ± 0.9	8.12 ± 0.00	1812 ± 4.3	1985 ± 3.6	246 ± 2.0	8.19 ± 0.00
HTHCLS	1938 ± 0.4	1997 ± 0.4	624 ± 0.2	7.83 ± 0.00	1912 ± 4.3	2004 ± 0.1	469 ± 17.5	7.95 ± 0.02
MR16-xp								
LT	1981 ± 3.1	1859 ± 2.4	276 ± 0.8	8.14 ± 0.00	1980 ± 2.0	1861 ± 3.1	279 ± 6.5	8.13 ± 0.01
LTHC	1966 ± 3.4	1956 ± 1.5	778 ± 21.0	7.71 ± 0.01	1966 ± 3.3	1953 ± 2.5	753 ± 12.6	7.73 ± 0.01
LTLS	1872 ± 3.7	1780 ± 2.0	311 ± 4.7	8.07 ± 0.01	1872 ± 1.2	1778 ± 1.6	306 ± 7.0	8.08 ± 0.01
LTHCLS	1866 ± 6.9	1859 ± 3.6	748 ± 33.7	7.71 ± 0.02	1872 ± 4.6	1855 ± 3.0	673 ± 12.0	7.76 ± 0.01
HT	1983 ± 5.4	1859 ± 2.4	331 ± 6.4	8.07 ± 0.01	1985 ± 11.8	1860 ± 0.6	333 ± 28.1	8.07 ± 0.04
HTHC	1954 ± 6.5	1930 ± 3.4	805 ± 26.2	7.71 ± 0.02	1957 ± 10.4	1926 ± 1.8	758 ± 63.1	7.74 ± 0.04
HTLS	1866 ± 4.8	1757 ± 3.7	329 ± 11.1	8.06 ± 0.01	1868 ± 2.7	1758 ± 4.0	323 ± 7.8	8.06 ± 0.01
HTHCLS	1870 ± 6.1	1841 ± 2.1	714 ± 27.8	7.75 ± 0.02	1872 ± 5.3	1835 ± 2.5	658 ± 33.7	7.78 ± 0.02

HC and LS represents high CO_2 and lower salinity treatment, respectively. Data represents mean ± range of duplicate incubations (MR15-exp.) or mean ±1SD of triplicate incubations (MR16-exp.) at incubation temperature and salinity (see text). Abbreviations: DIC, dissolved inorganic carbon; TA, total alkalinity; pCO_2, partial pressure of CO_2.

thereby preparing triplicates for each of the eight treatments in the MR16-exp. The difference in the number of replicates is the consequence of the different water tank volume between 2 years that the MR-15exp. tank cannot incubate 12 bags. The carbonate chemistry, salinity, and nutrients (NO_3: 4 μmol L^{-1}, PO_4: 0.25 μmol L^{-1}, and $Si(OH)_4$: 3 μmol L^{-1}, in final concentrations) of each bag were manipulated. The added nutrient levels were lower compared to those in the MR15-exp. because of the very low biomass of phytoplankton at the beginning of the experiment. Then, the seawater was incubated in two water tanks where the temperature was controlled by thermostatic circulators. In one tank, the temperature was set at the *in situ* temperature, which was approximately 2°C in both years; in the other tank, the temperature was set to approximately 5°C higher than the *in situ* temperature. The water tanks were covered with neutral density mesh to decrease surface irradiance by 50%, which mimics similar irradiance levels to the depth of seawater sample collection. Incubations lasted for 11 (for the HT series) and 15 (for the LT series) days in the MR15-exp., and for 7 (for the HT series) and 8 (for the LT series) days in the MR16-exp. It should be noted that we did not use data after day 8 of the HT series and day 13 of the LT series in the MR15-exp. because of the nutrient depletion; i.e., the duration of experiments analyzed in this study is similar.

Biological and Chemical Analyses

During the course of the experiment, the temperature and PAR of each water tank were monitored using thermistor and photodiode sensors (JFE Advantech Co., Ltd., Hyogo, Japan), respectively, at 10 min intervals. Temperature and salinity

data of the water column were obtained from CTD (model 9 plus, Sea-Bird Scientific, Bellevue, WA, United States), and the salinity in the incubation bags was measured using an Autosal 8400B salinometer (Guildline Instruments Ltd., Smiths Falls, ON, Canada) with International Association for the Physical Sciences of the Ocean (IAPSO) standard seawater (Kawano et al., 2006). Seawater samples for dissolved inorganic carbon (DIC) and total alkalinity (TA) were collected approximately every third day to estimate carbonate chemistry. Concentrations of DIC and TA were measured onboard with coulometry (Dickson et al., 2007) and spectrophotometry (Yao and Byrne, 1998), respectively. The precisions of the DIC and TA measurements were <1.5 and <2.0 μmol kg^{-1}, respectively, which were estimated from the means and standard deviations of the concentrations measured in the duplicates of the seawater. Accuracies of the DIC and TA measurements were checked using a custom-made working standard, which was traceable to certified reference materials distributed by the Scripps Institution of Oceanography (Dickson et al., 2003). Carbonate chemistry was estimated using the CO2SYS program (Lewis and Wallance, 1998). We estimated the fractions of seawater (f_{SW}), sea ice melt (f_{SIM}), and other freshwater (f_{OF}: meteoric water = riverine input + precipitation) in the seawater sample at the beginning of the experiment following the method of Yamamoto-Kawai et al. (2009) using salinity and potential alkalinity (TA + nitrate - ammonium) values. We applied the end-member values of SW, SIM, and OF used by Nishino et al. (2016) in their study of water mass characteristics in the Chukchi Sea. Samples for nutrients (NO_3, NO_2, NH_4, PO_4, and $Si(OH)_4$) and total chlorophyll-*a* (chl-*a*) were taken every day

during the MR15-exp. and every second day during the MR16-exp.; samples for chl-*a* were obtained by filtering ∼100 mL samples through GF/F filters under a gentle vacuum (<100 mm Hg). Size-fractionated chl-*a* samples were collected periodically (generally at 2–3 day intervals) in both experiments, filtering 300 mL of seawater sequentially using 10 μm pore size of polycarbonate filters and GF/F filters under a gentle vacuum. Nutrient samples were analyzed onboard using a QuAAtro-2 continuous flow analyzer (BL Tec KK, Osaka, Japan) using reference materials for nutrients in seawater (Aoyama et al., 2012). The chl-*a* samples were measured with fluorometry using a Turner Design 10-AU Fluorometer (Welschmeyer, 1994) after extraction with *N, N*-dimethylformamide for at least 24 h at −20°C in the dark (Suzuki and Ishimaru, 1990). To measure small phytoplankton traits (<∼10 μm), we used flow cytometry (EC800 Flowcytometry Analyzer, SONY Corp., Tokyo, Japan), which could quantify the number of cyanobacteria (*Synechococcus*), PicoE (<∼2 μm in diameter) and eukaryotic nanophytoplankton (NanoE, ∼2 to 10 μm in diameter). Seawater samples of 2 mL were fixed with neutralized formalin (0.4% v/v as formaldehyde in final conc.) and stored in an −80°C freezer until laboratory analysis on land. Prior to measurement, samples were thawed and sieved through a cell strainer (with 35 μm mesh) to prevent clogging. To distinguish between cell sizes, 2.0 μm Fluoresbrite YG beads (Polysciences, Inc., Warrington, PA, United States) were measured simultaneously with the samples. Forward- and side-angle light scattering was used to distinguish the PicoE and NanoE sizes. Cyanobacteria and other phytoplankton were distinguished using chl-*a* and phycobiliproteins fluorescence. The number of cryptophytes was not quantified with flow cytometry because it appeared to be very low. Samples for accessory pigment analysis with high-performance liquid chromatography (HPLC) were collected at the beginning, on day 2 for the HT series and on day 3 for the LT series, during the exponential growth phase (day 6 for the HT series and day 8 for the LT series) and the end of the experiment in the MR15-exp., and samples were collected at the beginning, on day 2 for the HT series, on day 3 for the LT series and at the end of the experiment in the MR16-exp. Seawater samples for HPLC were collected onto GF/F filters under a gentle vacuum, flash frozen in liquid nitrogen and stored in a deep freezer at −80°C until laboratory analysis on land. Accessory pigments on the filter were extracted using *N, N*-dimethylformamide, and sonication, and extracted samples were measured by HPLC following the method of van Heukelem and Thomas (Van Heukelem and Thomas, 2001; Fujiwara et al., 2014, 2018). We analyzed the data of the following nine pigments: peridinin (autotrophic dinoflagellate), fucoxanthin (e.g., diatoms and pelagophytes), 19′-butanoyloxyfucoxanthin (e.g., pelagophytes), 19′-hexanoyloxyfucoxanthin (e.g., haptophytes), chlorophyll-*b*, prasinoxanthin, and violaxanthin (e.g., chlorophytes and prasinophytes), alloxanthin (e.g., cryptophytes), and zeaxanthin (e.g., cyanobacteria) (Van Heukelem and Thomas, 2001; Tremblay et al., 2009; Fujiwara et al., 2014). Determination of algal classes with pigment analysis requires caution because some algae share pigments of different algal classes such as dinoflagellates (e.g., Takishita et al., 1999; Zapata et al., 2012).

Although previous studies successfully analyzed algal classes with pigment composition in the western Arctic Ocean (Fujiwara et al., 2014, 2018), a detailed analysis of algal pigments inhabiting the Arctic may be needed in the future. Samples for microscopic observations were collected at the beginning, during the exponential growth phase and at the end of the MR15-exp., and the samples were collected at the beginning and at the end of the experiment in the MR16-exp. Relatively larger phytoplankton, mainly diatoms (>∼10 μm), were enumerated in terms of cell number and volume, thereby calculations of cell density and biomass were performed using an inverted microscope under 100 × , 200 × or 400 × magnifications (Olympus Corp., Tokyo, Japan). Diatoms were identified at the species or genus level following Hasle and Syvertsen (1997). The cell volume was estimated based on the geometric similarity (Hillebrand et al., 1999) and then converted into carbon biomass using an allometric relationship (Menden-Deuer and Lessard, 2000). The diversity of diatoms was estimated by the Shannon-Weiner (*H*′) index using biomass data (Tuomisto, 2010; Sugie and Suzuki, 2015). The use of an index that is based on estimates of biomass and not abundance is particularly appropriate when organisms of interest have a large variability in size, such as diatoms (Sugie and Suzuki, 2015, 2017).

To estimate the specific growth rate (μ: d^{-1}), linear regression was applied between incubation day and the natural log of the size fractionated chl-*a* concentration or the abundance of *Synechococcus*, PicoE, and NanoE before nutrient depletion. For diatoms and accessory pigments, because there were few biomass measurements, specific growth rates were calculated using the following formula:

$$\mu = (\text{Ln}B_n - \text{Ln}B_m)/(n - m),$$

where B_n and B_m represent measured biomass at day n and m of incubation (n > m), respectively, before nutrient depletion.

Statistics

To test the impacts of changes in temperature, CO_2, and salinity on phytoplankton dynamics, stepwise multiple linear regression was used to detect the relationships between modified environmental perturbations and specific growth rates. Environmental variables examined in the multiple linear regression analysis were temperature (T), pH, salinity (S), T × pH, T × S, and pH × S to take into account interactive effects. Next, because all datasets passed the normality test, we analyzed the mean values of the measured specific growth rates among the different treated environmental perturbations with the Tukey-Kramer for one-way ANOVA test. In addition, three-way ANOVA was performed to check the interactive effects. Note that the factor of the interactive effect of T × pH × S was eliminated because of the multicolinearity in both multiple regression analyses and three-way ANOVA tests. The data were statistically analyzed using PASW Statistic software (version 17.0, SPSS Inc., Chicago, IL, United States) and Origin software (Lightstone Corp., Tokyo, Japan) and reported at the 95% confidence level. The results are shown as the mean ± range between two bottles

of duplicate incubations for the MR15-exp. and the mean ± 1 SD of triplicate incubations for the MR16-exp.

RESULTS

Initial Conditions of Incubations

At the beginning of the MR15-exp., the temperature, salinity and partial pressure of CO_2 (pCO_2) of the seawater used for the incubation experiments were 2.9°C, 29.2, and 294 μatm, respectively; in the MR16-exp., they were 2.6°C, 27.3, and 287 μatm, respectively. The physicochemical properties of the seawater in the two experiments were different; the fraction of sea ice melt water, f_{SIM} in the MR16-exp. (10.6%) was nearly twice that in the MR15-exp. (6.8%). Daily light availability during MR15-exp. (1.36 mol photon m^{-2} day^{-1}) was about 2.7 times lower than that during MR16-exp. (3.66 mol photon m^{-2} day^{-1}). Diurnal maximum PAR values were 40–150 and 100–340 μmol photon m^{-2} s^{-1} in MR15-exp. and MR16-exp., respectively. In the MR15-exp., the mean temperatures in the LT and HT series were 2.3 and 7.2°C, respectively; in the MR16-exp., they were 2.1 and 6.8°C. In the LS series, the salinity successfully decreased to 1.417 and 1.403, respectively, compared with those in the controls in the MR15-exp. and the MR16-exp. In the MR15-exp., the total chl-a concentration and the fraction of large-sized phytoplankton (>10 μm) were 1.0 μg L^{-1} and 43%, respectively; in the MR16-exp., they were 0.27 μg L^{-1} and 14%, respectively. In the MR15-exp., the dominant accessory pigment was fucoxanthin (27%), followed by chlorophyll-b (24%) and peridinin (10%); in the MR16-exp., the dominant accessory pigment was chlorophyll-b (48%), followed by fucoxanthin (11%) and 19′-hexanoyloxyfucoxanthin (7%). At the beginning of the MR15-exp., the abundances of *Synechococcus*, PicoE and NanoE were 530, 4900 and 670 cells mL^{-1}, respectively; in the MR16-exp., they were 73, 4500 and 1700 cells mL^{-1}, respectively. Diatom biomass in the MR15-exp. (0.17 μg C L^{-1}) was three times that in the MR16-exp. (0.053 μg C L^{-1}), whereas the diversity index was higher in the MR16-exp. (H' = 2.01) than in the MR15-exp. (H' = 1.50).

During the course of both experiments, pH and pCO_2 values exhibited a clear difference between the control CO_2 and HC series. At the beginning of the MR15-exp., the mean pH and pCO_2 of the control CO_2 series (the LT, LTLS, HT, and HTLS treatments) were 8.126 ± 0.011 and 299 ± 11 μatm, respectively; the mean pH and pCO_2 of the HC series (the LTHC, LTLSHC, HTHC, and HTLSHC treatments) were 7.834 ± 0.022 and 623 ± 48 μatm, respectively. At the beginning of the MR16-exp., the mean pH and pCO_2 in the control CO_2 series were 8.078 ± 0.034 and 315 ± 22 μatm, respectively, and those in the HC series were 7.716 ± 0.018 and 770 ± 42 μatm, respectively (**Table 1**). Increasing pH and decreasing pCO_2 levels were observed after a large nutrient drawdown occurred (i.e., phytoplankton growth) between days 5 and 8 in the HT series and between days 8 and 12 in the LT series in the MR15-exp., whereas such changes were absent in the MR16-exp. (**Supplementary Figure S2** and **Table 1**). The change in pH and pCO_2 was mainly driven by a decrease in DIC in the

incubation bags (**Table 1**). Overall, temperature, salinity, and carbonate chemistry manipulations in the different treatments were successful throughout the experiments.

Phytoplankton Growth

In the MR15-exp., chl-a concentrations reached a maximum at day 9 in the HT series and at day 16 in the LT series when nitrate was depleted (<0.1 μmol L^{-1}), whereas in the MR16-exp., ample nutrients remained, and phytoplankton growth continued until the end of experiment (**Supplementary Figures S2E, S3**). There were salient differences between the two experiments in phytoplankton size composition; during the exponential growth phase, the fraction of large-sized chl-a increased from 43% to >70% in the MR15-exp. but only from 14% to <30% in the MR16-exp. Multiple regression analysis and three-way ANOVA indicates that increased temperatures significantly enhanced the growth of phytoplankton in terms of chl-a in all size fractions in both experiments (**Table 2** and **Supplementary Table S1**). Higher CO_2 levels significantly enhanced the growth of phytoplankton in the smaller fraction of chl-a in both experiments with three-way ANOVA (**Supplementary Table S1**), but they did not affect the larger fraction of chl-a (**Figure 2**, **Table 2**, and **Supplementary Table S1**). Lower pH and salinity synergistically enhanced the phytoplankton growth in the fraction of small-sized chl-a in the MR15-exp. (**Figure 2** and **Table 2**). According to the standardizing coefficient of multiple regression analysis, the effect of temperature is larger than that of lower pH or pH × salinity on the specific growth rate of phytoplankton in the smaller fraction of chl-a (**Supplementary Table S2**).

Specific growth rates of diatoms were enhanced under increased temperature in both experiments (**Figures 3A,B** and **Table 2**). Although other factors significantly affected the diatom growth rates either in the multiple regression analysis or three-way ANOVA (**Table 2** and **Supplementary Table S1**), temperature is a prime factor on their growth (**Supplementary Table S2**). The growth of NanoE showed different patterns in the two experiments that the HT × HC and HC conditions significantly increased the specific growth rates of the MR15-exp. and MR16-exp., respectively (**Figures 3C,D** and **Table 2**). The three-way ANOVA detected the interactive effect in the MR15-exp. that the lower salinity levels depressed the growth of NanoE under higher CO_2 levels (**Figure 3C** and **Supplementary Table S1**). The PicoE did not show a positive growth in all tested conditions in the MR15-exp., whereas they were significantly enhanced by the HT and HC conditions in the MR16-exp. (**Figures 3E,F**, **Table 2**, and **Supplementary Table S1**). In both experiments, the increased temperature enhanced the specific growth rates of *Synechococcus* in the three-way ANOVA (**Supplementary Table S1**), and the growth rate showed a positive value only in the HT series (**Figures 3G,H**). In the species composition of diatoms, in terms of carbon biomass, the dominance of chain-forming diatoms such as *Thalassiosira* spp. decreased and that of elongated and solitary pennate diatoms *Cylindrotheca closterium* increased under the warmer conditions in the MR15-exp. (**Figure 4A**). According to the multiple regression analysis, the HT and LS conditions synergistically negative impact on the growth of chain-forming

TABLE 2 | Statistical results of multiple regression analysis between environmental variables (Temperature: T, pH, and Salinity: S) and the growth rate (μ) of phytoplankton and pigments. Listed are the coefficients of regression equation of $\mu = (a \times T) + (b \times pH) + (c \times S) + (d \times T \times pH) + (e \times T \times S) + (f \times pH \times S)$. Consistent trends between two culture experiments represented in bold.

Exp.	Component	a	b	c	d	e	f	Statistics
MR15	>10 µm Chl-a	**0.031 ± 0.003**	N.S.	N.S.	N.S.	N.S.	N.S.	$F_{1,14} = 124$, $p < 0.001$, $R^2 = 0.89$
	<10 µm Chl-a	**0.013 ± 0.002**	N.S.	N.S.	N.S.	N.S.	−0.0033 ± 0.0009	$F_{2,13} = 21.3$, $p < 0.001$, $R^2 = 0.73$
	Diatoms	**0.043 ± 0.002**	N.S.	N.S.	N.S.	N.S.	−0.0024 ± 0.0008	$F_{2,13} = 192$, $p < 0.001$, $R^2 = 0.96$
	Nano-E	N.S.	N.S.	N.S.	0.034 ± 0.000	N.S.	N.S.	$F_{1,14} = 103$, $p < 0.001$, $R^2 = 0.87$
	Pico-E	N.S.	N.S.	N.S.	N.S.	N.S.	N.S.	
	Synechococcus	N.S.	N.S.	N.S.	0.003 ± 0.000	N.S.	N.S.	$F_{1,14} = 249$, $p < 0.001$, $R^2 = 0.94$
	Ch. spp.	N.S.	N.S.	N.S.	N.S.	−0.0003 ± 0.0001	N.S.	$F_{1,14} = 17.1$, $p = 0.001$, $R^2 = 0.52$
	Th. spp.	N.S.	N.S.	N.S.	N.S.	**−0.0015 ± 0.0002**	N.S.	$F_{1,14} = 49.0$, $p < 0.001$, $R^2 = 0.76$
	Other centrics	N.S.	N.S.	N.S.	N.S.	N.S.	N.S.	
	C. closterium	N.S.	N.S.	N.S.	0.004 ± 0.000	N.S.	N.S.	$F_{1,14} = 36.1$, $p < 0.001$, $R^2 = 0.70$
	Ps. spp.	0.014 ± 0.003	N.S.	N.S.	N.S.	N.S.	N.S.	$F_{1,14} = 30.4$, $p < 0.001$, $R^2 = 0.66$
	Other pennates	N.S.	N.S.	N.S.	N.S.	N.S.	N.S.	
	Diatom diversity	N.S.	N.S.	N.S.	N.S.	−0.0018 ± 0.0005	N.S.	$F_{1,14} = 13.8$, $p = 0.002$, $R^2 = 0.46$
	Peridinin	N.S.	N.S.	N.S.	N.S.	0.0010 ± 0.0002	N.S.	$F_{1,14} = 40.3$, $p < 0.001$, $R^2 = 0.72$
	19′But.	N.S.	N.S.	N.S.	N.S.	0.0007 ± 0.0001	N.S.	$F_{1,14} = 17.1$, $p = 0.001$, $R^2 = 0.52$
	Fucoxanthin	0.030 ± 0.004	N.S.	N.S.	N.S.	N.S.	N.S.	$F_{1,14} = 69.3$, $p < 0.001$, $R^2 = 0.82$
	19′Hex.	0.042 ± 0.003	N.S.	N.S.	N.S.	N.S.	N.S.	$F_{1,14} = 238$, $p < 0.001$, $R^2 = 0.94$
	Prasinoxanthin	−0.014 ± 0.005	N.S.	N.S.	N.S.	N.S.	N.S.	$F_{1,14} = 7.47$, $p = 0.016$, $R^2 = 0.30$
	Violaxanthin	N.S.	N.S.	N.S.	0.002 ± 0.000	N.S.	N.S.	$F_{1,14} = 57.9$, $p < 0.001$, $R^2 = 0.80$
	Alloxanthin	N.S.	N.S.	N.S.	N.S.	N.S.	N.S.	
	Zeaxanthin	N.S.	N.S.	N.S.	N.S.	−0.0003 ± 0.0001	N.S.	$F_{1,14} = 5.58$, $p = 0.034$, $R^2 = 0.25$
	Chl-b	0.022 ± 0.002	N.S.	N.S.	N.S.	N.S.	N.S.	$F_{1,14} = 95.9$, $p < 0.001$, $R^2 = 0.86$
MR16	>10 µm Chl-a	**0.026 ± 0.002**	N.S.	N.S.	N.S.	N.S.	N.S.	$F_{1,21} = 109$, $p < 0.001$, $R^2 = 0.83$
	<10 µm Chl-a	**0.016 ± 0.002**	−0.104 ± 0.022	N.S.	N.S.	N.S.	N.S.	$F_{2,20} = 57.0$, $p < 0.001$, $R^2 = 0.84$
	Diatoms	**0.038 ± 0.002**	N.S.	N.S.	N.S.	N.S.	N.S.	$F_{2,20} = 563$, $p < 0.001$, $R^2 = 0.96$
	Nano-E	N.S.	−0.134 ± 0.040	N.S.	N.S.	N.S.	N.S.	$F_{1,21} = 11.3$, $p = 0.003$, $R^2 = 0.32$
	Pico-E	0.008 ± 0.003	−0.185 ± 0.038	N.S.	N.S.	N.S.	N.S.	$F_{2,20} = 16.7$, $p < 0.001$, $R^2 = 0.59$
	Synechococcus	0.050 ± 0.007	N.S.	N.S.	N.S.	N.S.	N.S.	$F_{1,21} = 52.4$, $p < 0.001$, $R^2 = 0.70$
	Ch. spp.	N.S.	N.S.	N.S.	N.S.	N.S.	N.S.	
	Th. spp.	N.S.	N.S.	N.S.	N.S.	**−0.0002 ± 0.0001**	N.S.	$F_{1,21} = 6.59$, $p = 0.018$, $R^2 = 0.20$
	Other centrics	N.S.	N.S.	N.S.	N.S.	N.S.	N.S.	
	C. closterium	N.S.	N.S.	N.S.	N.S.	N.S.	0.0039 ± 0.001	$F_{1,21} = 5.47$, $p = 0.029$, $R^2 = 0.17$
	Ps. spp.	N.S.	−0.086 ± 0.041	N.S.	N.S.	N.S.	N.S.	$F_{1,21} = 4.36$, $p = 0.049$, $R^2 = 0.13$
	Other pennates	N.S.	N.S.	N.S.	N.S.	N.S.	N.S.	
	Diatom diversity diversity	N.S.	N.S.	0.114 ± 0.049	N.S.	N.S.	N.S.	$F_{1,21} = 5.38$, $p = 0.030$, $R^2 = 0.16$
	Peridinin	−0.385 ± 0.090	N.S.	N.S.	N.S.	0.016 ± 0.003	N.S.	$F_{2,20} = 39.1$, $p < 0.001$, $R^2 = 0.78$
	19′But.	N.S.	−0.141 ± 0.037	N.S.	N.S.	0.0006 ± 0.0001	N.S.	$F_{2,20} = 25.2$, $p < 0.001$, $R^2 = 0.69$
	Fucoxanthin	N.S.	−0.093 ± 0.034	0.019 ± 0.008	N.S.	0.0013 ± 0.0001	N.S.	$F_{3,19} = 79.8$, $p < 0.001$, $R^2 = 0.92$
	19′Hex.	N.S.	N.S.	N.S.	N.S.	0.0009 ± 0.0001	0.0033 ± 0.0009	$F_{2,20} = 34.5$, $p < 0.001$, $R^2 = 0.75$

(Continued)

TABLE 2 | Continued

Exp.	Component	a	b	c	d	e	f	Statistics
	Prasinoxanthin	0.016 ± 0.005	−0.370 ± 0.061	N.S.	N.S.	N.S.	N.S.	$F_{2,20} = 24.9$, $p < 0.001$, $R^2 = 0.69$
	Violaxanthin	0.015 ± 0.003	N.S.	N.S.	N.S.	N.S.	−0.0046 ± 0.001	$F_{2,20} = 19.2$, $p < 0.001$, $R^2 = 0.62$
	Alloxanthin*	0.0006 ± 0.000	N.S.	N.S.	N.S.	N.S.	N.S.	$F_{1,21} = 57.7$, $p < 0.001$, $R^2 = 0.72$
	Zeaxanthin	−0.247 ± 0.100	−0.275 ± 0.072	N.S.	N.S.	0.0100 ± 0.0037	N.S.	$F_{3,19} = 12.4$, $p < 0.001$, $R^2 = 0.61$
	Chl-b	N.S.	−0.136 ± 0.037	N.S.	N.S.	0.0009 ± 0.0001	N.S.	$F_{2,20} = 40.8$, $p < 0.001$, $R^2 = 0.78$

N.S., not significant. Abbreviations: Chl-a, Chlorophyll-a; Nano-E, nano-sized eukaryotic phytoplankton; Pico-E, pico-sized eukaryotic phytoplankton; Ch., Chaetoceros; Th., Thalassiosira; Ps., Pseudo-nitzschia; 19'But., 19'-buanoiloxifucoxanthin; Chl-b, chlorophyll-b; 19'Hex., 19'-hexanoiloxifucoxanthin; N.S., not significant. *Alloxanthin in MR16-exp. we analyzed using concentration data at the end of incubation (day 6 and 7 for LT and HT series, respectively). We could not estimate specific growth rate properly due to extremely low concentration in days 2 or 3.

Chaetoceros spp. in the MR15-exp. and *Thalassiosira* spp. in both experiments (**Table 2**). In the MR15-exp., the HT and the HT × HC conditions enhanced the growth rate of *Pseudo-nitzschia* spp. and *C. closterium*, respectively (**Table 2**). In the MR16-exp., the growth rate of *Pseudo-nitzschia* spp. was enhanced under the HC conditions (**Figure 4B** and **Table 2**). The diversity index of diatoms was generally higher in the MR16-exp. community than in the MR15-exp. community (**Figures 4A,B**). The HT × LS conditions in the MR15-exp. and the LS conditions in the MR16-exp. were associated with a significant decrease in the diversity index (**Table 2** and **Supplementary Table S1**).

In MR15-exp., the specific growth rates of almost all phytoplankton traits estimated from pigment concentrations except prasinoxanthin and zeaxanthin containing algae were enhanced under increased temperature or the combination of the HT and control salinity conditions (**Figure 5**, **Table 2**, and **Supplementary Table S1**). Notably, the growth rates of algae containing chlorophyll-*b* and violaxanthin (green algae) as well as algae containing 19′-hexanoyloxyfucoxanthin (e.g., Haptophyceae) showed positive values only under warmer conditions. In the MR16-exp., higher temperatures or the combination of the HT and control salinity conditions significantly enhanced all phytoplankton growth rates estimated from pigments (**Figure 6** and **Table 2**). The growth rates of algae containing peridinin showed positive values only under the HT conditions (**Figure 6B**). Alloxanthin concentration can be quantified only at the end of the HT series (**Figure 6I**). In addition, higher CO_2 levels significantly enhanced the growth of most of the algae except peridinin, alloxanthin and 19′-hexanoyloxyfucoxanthin containing one (**Table 2** and **Supplementary Table S1**). The HC and HT levels individually enhanced the growth of prasinoxanthin containing algae and the impact of the HC levels was about twice stronger than the HT levels (**Figure 6E**, **Table 2**, **Supplementary Tables S1**, **S2**). The synergistic effects of higher temperature and lower salinity were significant in some pigments that were diminished (peridinin, 19′-butanoyloxyfucoxanthin, fucoxanthin, 19′-hexanoyloxyfucoxanthin, zeaxanthin and chlorophyll-*b*) (**Table 2**). The growth rate of violaxanthin containing algae was significantly enhanced due to higher temperature and the combined effect of HC and LS levels (**Figure 6F**, **Table 2**, and **Supplementary Table S1**).

To explore the functional groups that are representative of each size fraction of chl-*a*, we performed factorial analysis of the relationships between the specific growth rates as estimated from size-fractionated chl-*a* and accessory pigments (**Supplementary Figures S4**, **S5** and **Supplementary Table S3**). For example, the slope and intercept of the regression line relative to the 1:1 line indicate that fucoxanthin containing algae (likely diatoms) was dominant in the >10 μm fraction of chl-*a* in both experiments (**Supplementary Figures S4C-1, S5C-1**). Many algae containing, such as peridinin, 19′-butanoyloxyfucoxanthin and 19′-hexanoyloxyfucoxanthin, contributed to chl-*a* in the small-size fraction in both experiments (**Supplementary Figures S4A-2, S4B-2, S4D-2, S5A-2, S5B-2, and S5D-2**). Although significant linearity exists between the specific growth rate of chl-*a*
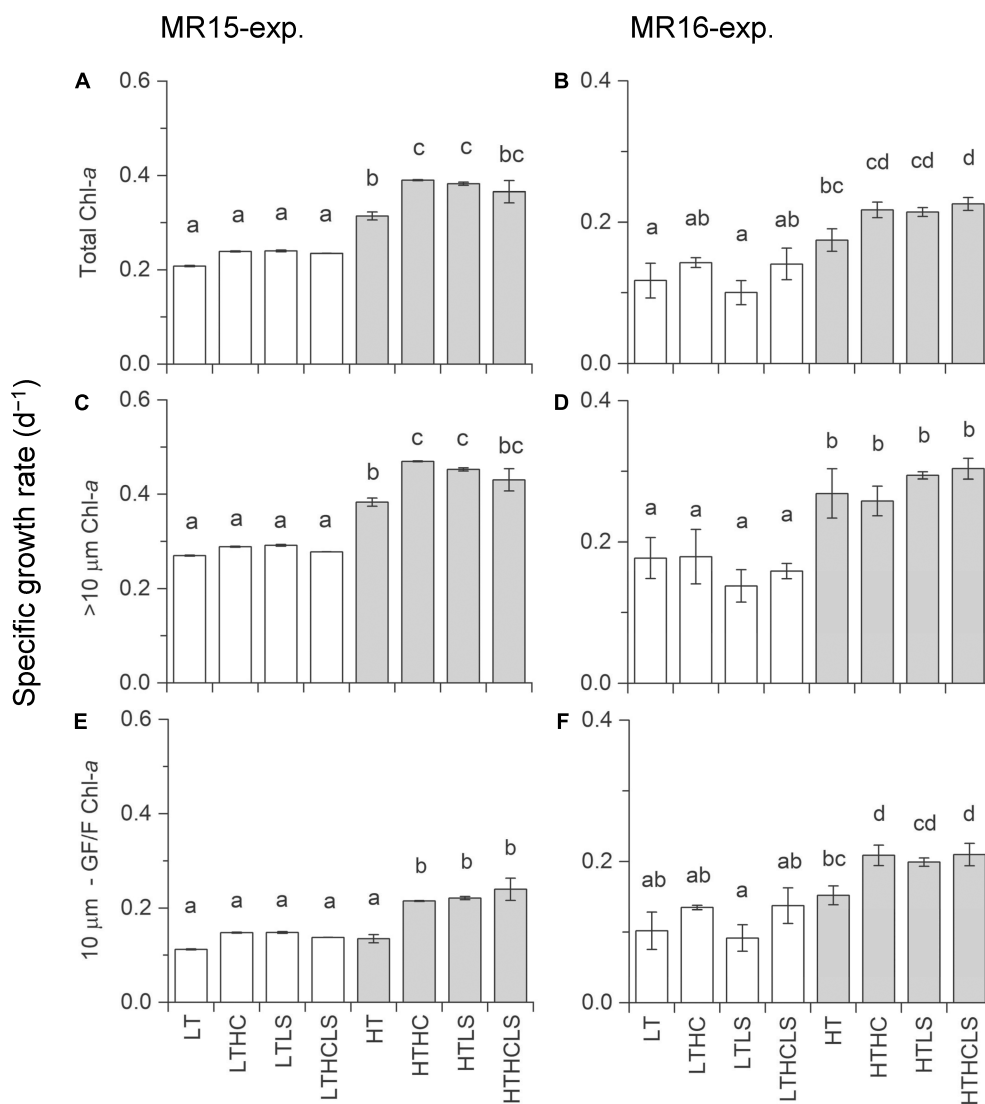
FIGURE 2 | Specific growth rates based on chlorophyll-*a* concentrations during the exponential growth phase. Left and right panels represent the MR15-exp. and the MR16-exp., respectively. **(A,B)** total chl-*a*, **(C,D)** >10 μm size fraction, and **(E,F)** <10 μm sized fraction. Letters above the bars represent statistical results of groups according to the Tukey–Kramer test.

in both size fractions and of violaxanthin and chlorophyll-*b* (i.e., green algae), the line's lower position and negative intercept relative to the 1:1 line indicate that green algae were a rather minor component in the phytoplankton community in the MR15-exp. (**Supplementary Figures S4F-2, S4I-2**). In contrast, in the MR16-exp., green algae may be one of the most dominant components of the small size fraction together with the algae containing peridinin, 19′-hexanoyloxyfucoxanthin, 19′-butanoyloxyfucoxanthin and zeaxanthin (**Supplementary Figures S5F-2, S5H-1**). The relationship of the results between microscopy and pigment analysis indicates that diatoms largely contributed fucoxanthin in both experiments (**Supplementary Figures S4C-3, S5C-3**). Peridinin, 19′-butanoyloxyfucoxanthin and 19′-hexanoyloxyfucoxanthin correlated with NanoE in the MR15-exp. (**Supplementary Figures S4A-4, S4B-4, and**

S4D-4 and Supplementary Table S3). In the MR16-exp., the relationship between PicoE and chlorophyll-*b*, between PicoE and prasinoxanthin and between PicoE and violaxanthin are closely related to the 1:1 line (**Supplementary Figures S5E-5, S5F-5, and S5H-5** and **Supplementary Table S3**).

DISCUSSION

This study demonstrated the effect of changes in temperature, CO_2 and salinity on phytoplankton communities in the shelf edge area of the western Arctic Ocean where lateral transport of organic carbon to the deeper Canada Basin occurs (Watanabe et al., 2014; Harada, 2016). The impact of higher temperature enhanced the growth of most phytoplankton traits,

FIGURE 3 | Specific growth rate of **(A,B)** diatom biomass, **(C,D)** eukaryotic nanophytoplankton, **(E,F)** eukaryotic nanophytoplankton, and **(G,H)** *Synechococcus*. Left and right panels represent the MR15-exp. and the MR16-exp., respectively. Letters above the bars represent statistical results of groups according to the Tukey–Kramer test.
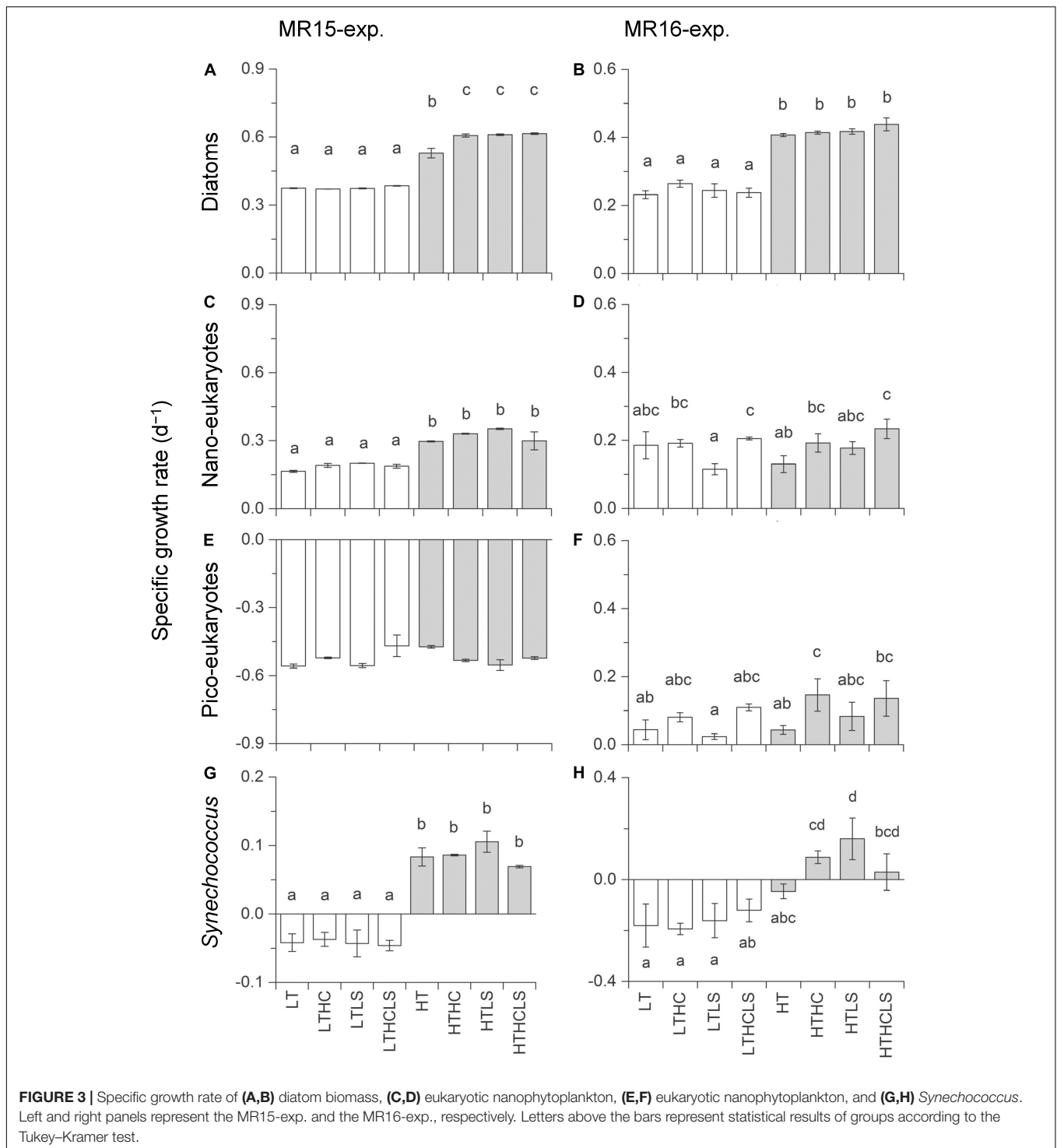
and higher CO_2 and lower salinity affected phytoplankton traits differently or between experiments. We found that some phytoplankton traits exhibited a positive specific growth rate only after the perturbation of temperature (algae containing violaxanthin and chlrophyll-*b* in the MR15-exp. and containing 19′-hexanoyloxyfucoxanthin, peridinin and alloxanthin in the MR16-exp., and *Synechococcus* in both experiments)

or under the combination of high CO_2 and temperature (prasinoxanthin containing algae in the MR16-exp.). The impact of lower salinity was marginal but significantly decreases the growth of chain-forming *Thalassiosira* spp. and diatom diversity (**Table 2** and **Supplementary Table S1**). These results suggest that these environmental conditions play key roles in phytoplankton dynamics in the western Arctic Ocean. Notably,

FIGURE 4 | Community composition and diversity index of diatoms in **(A)** the MR15-exp. and **(B)** the MR16-exp. during the exponential growth phase. Black circle and error bars represent the mean of Shannon index and error range or 1SD of duplicate (MR15-exp.) or triplicate (MR16-exp.) incubations.
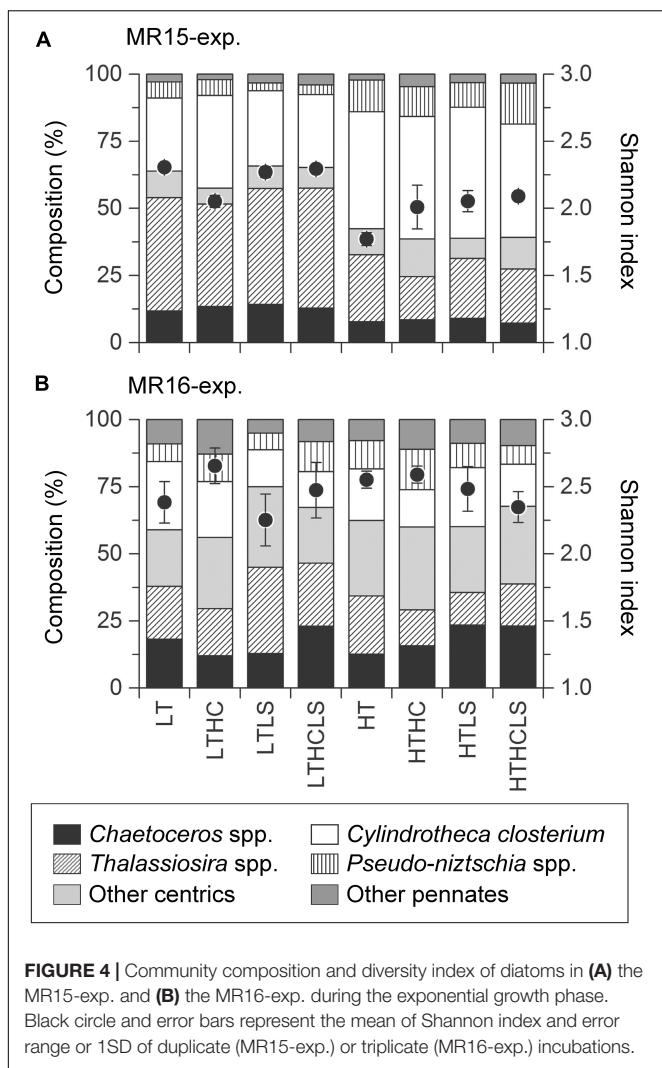
the environmental perturbations led to an increase in the growth of small-sized phytoplankton groups in both experiments and non-chain-forming diatoms in the MR15-exp. Although the composition of the initial phytoplankton community and seawater physicochemical properties, in particular f_{SIM}, were substantially different between the two experiments, this study suggests that recent and probably future Arctic changes, such as warming, acidification, and freshening can potentially modify the phytoplankton community to decrease the carbon export efficiency as well as energy transfer to higher trophic levels (Marañón, 2015) and can potentially weaken the coupling between the pelagic and benthic food webs (Grebmeier et al., 2015).

Some temperature and/or CO_2 manipulation experiments have been performed in the eastern Arctic Ocean (Schulz et al., 2013; Coello-Camba et al., 2014; Thoisen et al., 2015; Hussherr et al., 2017; Hoppe et al., 2018c,b; Wolf et al., 2018). Although a few experiments reported that higher CO_2 levels did not affect the productivity and photophysiology of phytoplankton communities (Hoppe et al., 2018a,b,c; Wolf et al., 2018), one

of the consistent results is that the growth rate or abundance of PicoE increased under high CO_2 levels in the Arctic Ocean (Schulz et al., 2013; Hussherr et al., 2017, MR16-exp. of this study). Such a positive effect of high CO_2 levels on the growth of PicoE communities has also been reported in the temperate coastal regions of Europe, the oceanic subarctic Pacific, and the Southern Ocean (Meakin and Wyman, 2011; Yoshimura et al., 2014; Davidson et al., 2016; Schulz et al., 2017 and references therein). Furthermore, this study demonstrated for the first time the enhancement of the growth of PicoE because of the interactive (MR16-exp.) or individual (MR15-exp.) effects of higher CO_2 and higher temperature using Arctic phytoplankton communities (**Table 2** and **Supplementary Table S1**). In a unialgal culture, *Micromonas pusilla*, one of the most dominant PicoE species in the Arctic Ocean (Lovejoy et al., 2007; Tremblay et al., 2009), responded positively to both CO_2 and higher temperature conditions (Hoppe et al., 2018a). Previous studies have suggested that the possible underlying mechanism of higher growth performance of PicoE under high CO_2 conditions (i.e., high aqueous CO_2 concentration) is that the uptake of DIC by PicoE may rely largely on molecular diffusion of aqueous CO_2 rather than active HCO_3^- transport via carbonic anhydrase (Schulz et al., 2017; Hoppe et al., 2018a); higher temperature further enhances the efficiency of electron transport by increasing the turnover rates of the CO_2-fixing enzyme RubisCO (Mock and Hoch, 2005; Hoppe et al., 2018a). These previous studies are in line with our findings that PicoE, most probably prasinophytes, in the MR16-exp. (**Supplementary Figure S5E-5**) may increase the dominance in phytoplankton communities of the western Arctic Ocean under high temperature and CO_2 conditions. However, caution is needed to extrapolate the results of this study to the natural Arctic Ocean ecosystem because some results between the MR15-exp. and the MR16-exp. were different.

Impacts of high CO_2 levels on phytoplankton communities often differed between previous studies as well as between the MR15-exp. and the MR16-exp. This inconsistency may be largely a result of the phytoplankton community composition (Eggers et al., 2014; Richier et al., 2014; Yoshimura et al., 2014; Schulz et al., 2017), in particular, of relatively large intra- and interspecific variations (e.g., Langer et al., 2006, 2009; Schaum et al., 2013; Sugie et al., 2018; Wolf et al., 2018 and references therein). Throughout the experiments conducted in this study, the contributions of large phytoplankton groups as measured by size-fractionated chl-*a* and diatom biomass were several times higher in the MR15-exp. than in the MR16-exp. (**Supplementary Figures S3C,D**). However, competition between groups of large and small phytoplankton may not be responsible for this phenomenon because the specific growth rates of phytoplankton in the small-sized fraction of chl-*a* from the same treatment in the two experiments were relatively similar. Pigment analysis shows that each algal group responded differently to environmental perturbations between the two experiments, suggesting that the species composition of PicoE, and probably NanoE, were different in the experiments (**Figures 5**, **6**). Unfortunately, we did not further identify the species composition of the PicoE and NanoE communities with microscopy and HPLC. Molecular

FIGURE 5 | Specific growth rates based on the concentrations of **(A)** fucoxanthin, **(B)** peridinin, **(C)** zeaxanthin, **(D)** chlorophyll-*b*, **(E)** prasinoxanthin, **(F)** violaxanthin, **(G)** 19′-butanoyloxyfucoxanthin, **(H)** 19′-hexanoyloxyfucoxanthin, and **(I)** alloxanthin in the MR15-exp. Letters above the bars represent statistical results of groups according to the Tukey–Kramer test.
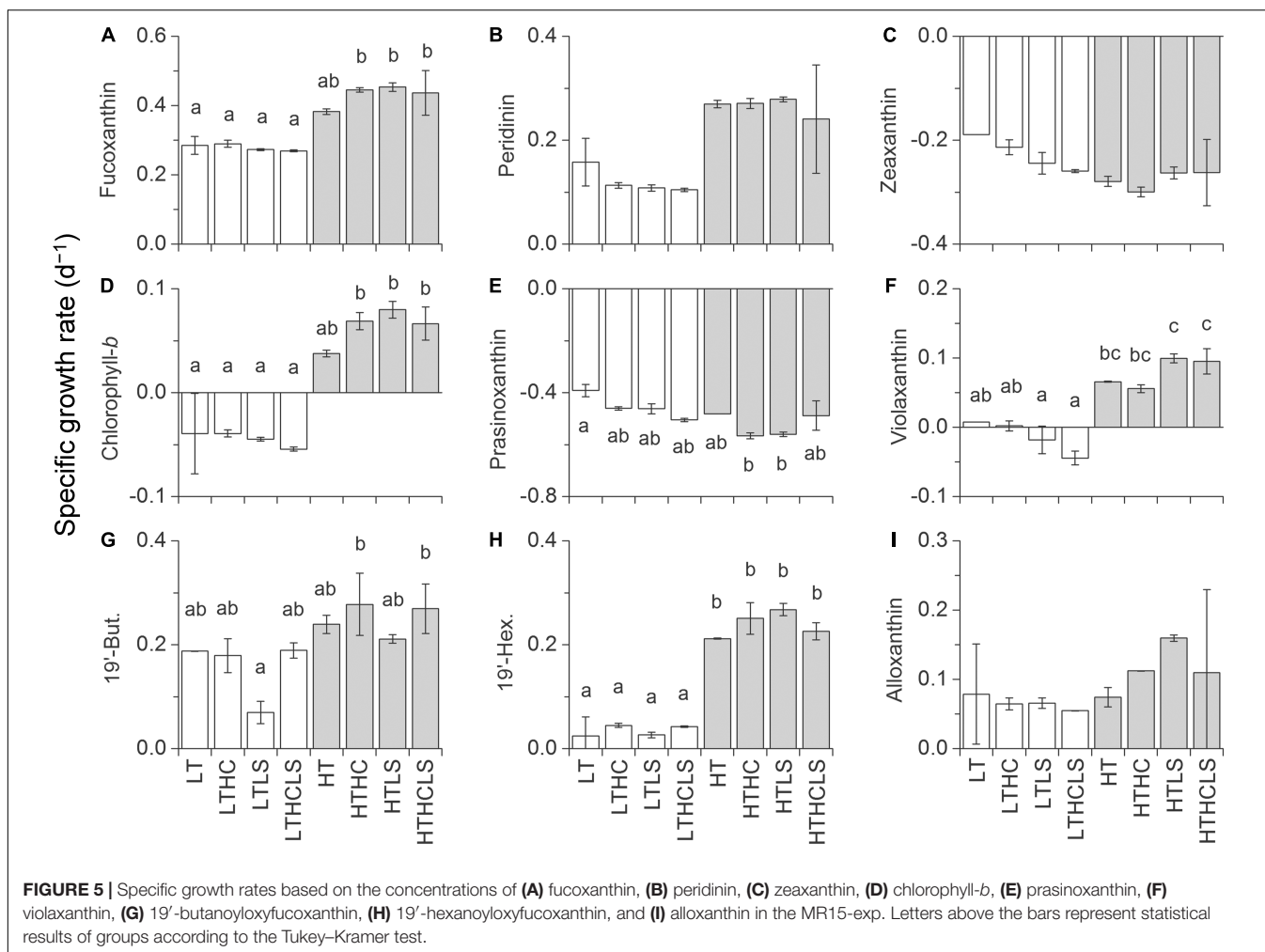
techniques are needed to achieve a better understanding of the impacts of environmental perturbations on small-sized plankton communities. Microzooplankton grazing is another important factor affecting PicoE and NanoE communities and was left unexplored in this study. Previous studies reported that microzooplankton grazing was not affected by high CO_2 levels (Aberle et al., 2013; Brussaard et al., 2013). Because temperature sensitivity is higher in microzooplankton than in phytoplankton, as estimated from laboratory culture experiments (Rose and Caron, 2007), microzooplankton grazing potentially outcompetes phytoplankton biomass at higher temperatures. However, the net specific growth rates of most of the algae increased under higher temperatures in this study, indicating that the relatively lower temperature in the HT series (ca. 7°C) still suppresses the microzooplankton grazing rate (Irigoien et al., 2005; Rose and Caron, 2007) or food limitation, i.e., lower phytoplankton biomass for microzooplankton compared to those in laboratory conditions in the western Arctic Ocean in September. Although there is room for further investigation, microzooplankton grazing is unlikely to be a major factor that shapes the specific growth rates of PicoE and NanoE under different temperature, CO_2 and salinity conditions.

The diversity of diatoms was decreased by the combination of higher temperature and lower salinity in the MR15-exp. and by lower salinity levels in the MR16-exp. At the beginning of the experiment, diatom diversity was higher in the MR16-exp. than in the MR15-exp., suggesting that diversity is an important factor in resisting or buffering the effects of environmental perturbations such as temperature in phytoplankton community composition. Previous studies suggested that intraspecific variability of sensitivity to high CO_2 conditions is one of the important factors that determines the stability of phytoplankton productivity (Hoppe et al., 2017, 2018c,b; Wolf et al., 2018). In this study, *C. closterium* appeared in both experiments. The difference observed in the two experiments may come from intraspecific variability or the differences in functional redundancy within a community (Hoppe et al., 2017; Wolf et al., 2018). We found that the lower salinity conditions can decrease diatom diversity in both experiments (**Table 2** and **Supplementary Table S1**), due to the decrease in chain-forming species and the increase in pennate species under higher temperature levels. These results indicate that when freshwater input such as sea ice melt occurs simultaneously with the other environmental perturbations, the only 1.4 unit change in

FIGURE 6 | The same figure style as that of **Figure 5** but for the MR16-exp. except with **(I)** alloxanthin, which shows pigment concentration at the end of the culture (days 7 and 8 for the HT and LT series, respectively).
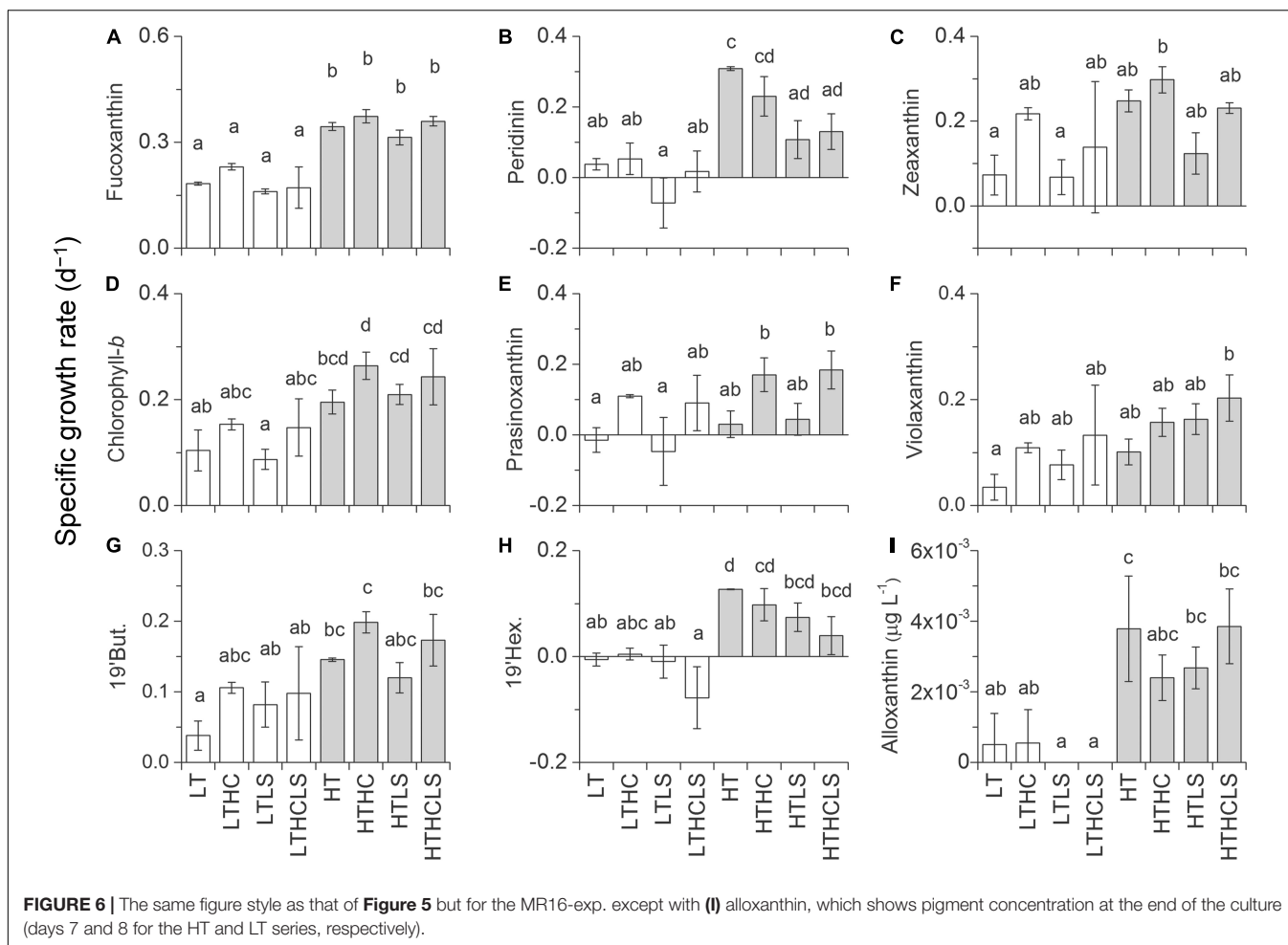
salinity has an important role in the ecosystem function of the western Arctic Ocean.

This is the first study that examined the simultaneous effects of changes in salinity, temperature and CO_2 on phytoplankton communities in the western Arctic Ocean. The results from biomass production of chl-a, microscopy, NanoE, and PicoE indicate that the effect of ∼1.4 lower salinity was rather small compared with that of approximately 5°C higher temperature and 300–450 μatm higher pCO_2 changes. However, note that the growth rates of many algal groups were influenced by the interactive effects of salinity and temperature or CO_2 rather than that of salinity alone as elicited by multiple regression analysis (**Table 2**). These results suggest that the effects of salinity or changing osmotic pressure on phytoplankton physiology interact with the change in temperature and/or CO_2, which is a contrast to the previous study that the effects of salinity and other environmental perturbations on phytoplankton ecophysiology are additive (Arrigo and Sullivan, 1992). In addition, the trends of the interactive effects of temperature and salinity, and CO_2 and salinity differed between phytoplankton lineages, probably due to the difference in the optimum temperature and salinity conditions. It has been reported that the optimum salinity conditions for phytoplankton growth are phytoplankton group

specific (e.g., Brand, 1984), even within a genus; i.e., they are species specific (*Heterocapsa* spp.: Yamaguchi et al., 1997; *Prymnesium* spp.: Larsen and Bryant, 1998; *Pseudo-nitzschia* spp.: Thessen et al., 2005; *Skeletonema* spp.: Balzano et al., 2011). Many previous studies suggested that salinity gradient in the estuary systems in temperate to tropical regions potentially modify phytoplankton community composition due to the difference in optimum salinity (e.g., Yamaguchi et al., 1997; Földer et al., 2010; Balzano et al., 2011). The detailed physiological experiment is required to clarify the interactive effects of salinity and the other environmental perturbations using Arctic phytoplankton communities or the unialgal culture of Arctic species. In the Arctic Ocean, decreasing salinity and expansion of low-salinity areas are expected because of the increase in sea ice melt and freshwater convergence (Comiso et al., 2008; Koenigk et al., 2013; Proshutinsky et al., 2015). This study finds that decreasing salinity can potentially modify phytoplankton community composition in the western Arctic Ocean under simultaneous change in temperature or CO_2 levels.

The effect of higher temperature was often consistent between the two experiments that enhanced the growth of many phytoplankton traits and depressed the growth of chain-forming diatom species (**Table 2**). The salient difference in the results

between the two experiments is the effect of higher CO_2 levels on the growth dynamics of phytoplankton (**Table 2**). Previous studies conducted in the subtropical to temperate coastal region and using the unialgal culture of model diatom species reported that the fertilization effects of higher CO_2 levels on phytoplankton growth can diminish with increasing irradiance levels (Gao et al., 2012, 2017; Li and Campbell, 2013). Negative interactive effect of higher CO_2 and light levels on two Antarctic diatom isolates have observed but it was not evident for prymnesiophyte *Phaeocystis antarctica* (Trimborn et al., 2017). In contrast, higher light intensity diminished the negative impact of high CO_2 levels on the productivity of Antarctic phytoplankton community (Heiden et al., 2019). In the present study, although the PAR levels were about three times higher in the MR16-exp., the fertilization effect of higher CO_2 levels on the growth rate of many non-diatom phytoplankton appeared only in the MR16-exp. (**Table 2**). These results suggest that the interactive effect of higher CO_2 and light levels on photophysiological processes varied between phytoplankton communities in the respective regions, and thereby that is not an important factor affecting phytoplankton dynamics in the western Arctic Ocean during autumn. We conclude that the difference in species composition, diversity, as well as intraspecific variability or functional redundancy as reported previously (Yoshimura et al., 2014; Hoppe et al., 2017, 2018c,b; Wolf et al., 2018), are important factors determining the impact of CO_2 levels in the western Arctic Ocean.

CONCLUSION

This study demonstrated that the interactive effects of higher CO_2, higher temperature and lower salinity can alter phytoplankton community composition in the western Arctic Ocean. Although the two experiments did not provide completely consistent results, higher temperature potentially increases the growth of almost all phytoplankton traits, whereas higher temperature and lower salinity synergistically decreases the contribution of chain-forming diatoms, such as *Thalassiosira* spp. (in both experiments), with decreasing diatom diversity. Higher CO_2 levels alone or the combination of higher CO_2 and lower salinity levels can enhance the growth of small-sized phytoplankton in terms of chl-*a* (in both experiments), especially of non-diatoms as measured pigments in the MR16-exp. (**Table 2**). Lower salinity enhances the growth of small-sized phytoplankton (in the MR-15-exp.) or leads to decreases in fucoxanthin-containing algae and diatom diversity in the MR16-exp., which were the major constituents of large-sized phytoplankton (**Table 2** and **Supplementary Figure S5C-1**). The results were consistent with those of many previous studies showing that the impact of higher temperature and/or CO_2 levels often enhances the growth of small-sized phytoplankton (Hare et al., 2007; Feng et al., 2009; Meakin and Wyman, 2011; Yoshimura et al., 2014; Davidson et al., 2016; Schulz et al., 2017). These results indicate decreasing biological carbon pumps, trophic transfer efficiency and food supply for benthos in the western Arctic Ocean under multiple environmental perturbations. Recent time-series observations indicate that smaller phytoplankton (PicoE) tend to dominate in the Arctic Ocean because of a decrease in nutrient availability as a result of stronger stratification induced by increased ice melt (Li et al., 2009; Ardyna et al., 2017). Our results indicate that under rapid environmental changes, such as warming, increased CO_2 levels, and freshening of the Arctic Ocean (Comiso et al., 2008; AMAP, 2013; Overland et al., 2014), the dominance of PicoE is likely to further increase. Although extrapolation of the results of this study to the Arctic ecosystem over a large scale and the long term requires caution, we conclude that phenotypic response to multiple environmental perturbations is one of the important elements in the ecosystem processes in the Chukchi Sea of the western Arctic Ocean.

DATA AVAILABILITY STATEMENT

All data used in this study will be available in the PANGAEA data depository for incubation (https://doi.org/10.1594/PANGAEA.899515) and the Data and Sample Research System for Whole Cruise Information (DARWIN) at http://www.godac.jamstec.go.jp/darwin/cruise/mirai/mr15-03_leg1/e and http://www.godac.jamstec.go.jp/darwin/cruise/mirai/mr16-06/e for environment.

AUTHOR CONTRIBUTIONS

KS and NH conceived and designed the experiments. KS, AF, and SK performed the onboard experiment. KS and AF measured and analyzed the data. KS wrote the manuscript with support from AF, SN, SK, and NH.

FUNDING

ACKNOWLEDGMENTS

SUPPLEMENTARY MATERIAL

The Supplementary Material for this article can be found online at: https://www.frontiersin.org/articles/10.3389/fmars.2019.00821/full#supplementary-material

REFERENCES

Aberle, N., Schulz, K. G., Stuhr, A., Malzahn, A. M., Ludwig, A., and Riebesell, U. (2013). High tolerance of microzooplankton to ocean acidification in an Arctic coastal plankton community. *Biogeosciences* 10, 1471–1481. doi: 10.5194/bg-10-1471-2013

AMAP, (2013). *AMAP Assessment 2013: Arctic Ocean Acidification, Arctic Monitoring and Assessment Programme*. Oslo: AMAP.

Aoyama, M., Ota, H., Kimura, M., Kitao, T., Mitsuda, H., Murata, A., et al. (2012). Current status of homogeneity and stability of the reference materials for nutrients in seawater. *Anal. Sci.* 28, 911–916. doi: 10.2116/analsci.28.911

Ardyna, M., Babin, M., Devred, E., Forest, A., Gosselin, M., Raimbault, P., et al. (2017). Shelf-basin gradients shape ecological phytoplankton nitches and community composition in the coastal Arctic Ocean (Beaufort Sea). *Limnol. Oceanogr.* 62, 2113–2132. doi: 10.1002/lno.10554

Ardyna, M., Babin, M., Gosselin, M., Devred, E., Rainville, L., and Tremblay, J. E. (2014). Recent Arctic Ocean sea ice loss triggers novel fall phytoplankton blooms. *Geophys. Res. Lett.* 41, 6207–6212. doi: 10.1002/2014gl061047

Arrigo, K. R., and Sullivan, C. W. (1992). The influence of salinity and temperature covariation on the photophysiological characteristics of Antarctic sea ice microalgae. *J. Phcol.* 28, 746–756. doi: 10.1111/j.0022-3646.1992.00746.x

Arrigo, K. R., and van Dijken, G. L. (2011). Secular trends in Arctic Ocean net primary productivity. *J. Geophys. Res.* 116:C09011. doi: 10.1029/2011JC007151

Balzano, S., Sarno, D., and Kooistra, W. H. C. F. (2011). Effects of salinity on the growth rate and morphology of ten *Skeletonema* strains. *J. Plankton Res.* 33, 937–945. doi: 10.1093/plankt/fbq150

Boyd, P. W., Dillingham, P. W., McGraw, C. M., Armstrong, E. A., Cornwall, C. E., Feng, Y.-Y., et al. (2016). Physiological responses of a Southern Ocean diatom to complex future ocean conditions. *Nat. Clim. Change* 6, 207–213. doi: 10.1038/nclimate2811

Brand, L. E. (1984). The salinity tolerance of forty-six marine phytoplankton isolates. *Estuar. Coast. Shelf Sci.* 18, 543–556. doi: 10.1016/0272-7714(84)90089-1

Brussaard, C. P. D., Noordeloos, A. A. M., Witte, H., Collenteur, M. C. J., Schulz, K., Ludwig, A., et al. (2013). Arctic microbial community dynamics influenced by elevated CO_2 levels. *Biogeosciences* 10, 719–731. doi: 10.5194/bg-10-719-2013

Coello-Camba, A., Agustí, S., Holding, J., Arrieta, J. M., and Duarte, C. M. (2014). Interactive effect of temperature and CO2 increase in Arctic phytoplankton. *Front. Mar. Sci.* 1:49. doi: 10.3389/fmars.2014.00049

Comiso, J. C., Parkinson, C. L., Gersten, R., and Stock, L. (2008). Accelerated decline in the Arctic sea ice cover. *Geophys. Res. Lett.* 35:L01703. doi: 10.1029/2007GL031972

Coupel, P., Ruiz-Pino, D., Sicre, M. A., Chen, J. F., Lee, S. H., Schiffrine, N., et al. (2015). The impact of freshening on phytoplankton production in the Pacific Arctic Ocean. *Prog. Oceanogr.* 131, 113–125. doi: 10.1016/j.pocean.2014.12.003

Davidson, A. T., McKinlay, J., Westwood, K., Thomson, P. G., van den Enden, R., de Salas, M., et al. (2016). Enhanced CO_2 concentrations change the structure of Antarctic marine microbial communities. *Mar. Ecol. Prog. Ser.* 552, 93–113. doi: 10.3354/meps11742

Dickson, A. G., Afghan, J. D., and Anderson, G. C. (2003). Reference materials for oceanic CO2 analysis: a method for the certification of total alkalinity. *Mar. Chem.* 80, 185–197. doi: 10.1016/s0304-4203(02)00133-0

Dickson, A. G., Sabine, C. L., and Christian, J. R. (2007). *Guide to Best Practices for Ocean CO2 Measurements PICES*. Washington, DC: Special Publications, 3.

Doney, S. C., Fabry, V. J., Feely, R. A., and Kleypas, J. A. (2009). Ocean acidification: the other CO_2 problem. *Annu. Rev. Mar. Sci.* 1, 169–192.

Edwards, K. F., Lichman, E., and Klausmeier, C. A. (2013). Functional traits explain phytoplankton community structure and seasonal dynamics in a marine ecosystem. *Ecol. Lett.* 16, 56–63. doi: 10.1111/ele.12012

Eggers, S. L., Lewandowska, A. M., Barcelos e Ramos, J., Blanco-Ameijeiras, S., Gallo, F., and Matthiessen, B. (2014). Community composition has greater impact on the functioning of marine phytoplankton communities than ocean acidification. *Glob. Change Biol.* 20, 713–723. doi: 10.1111/gcb.12421

Feng, Y., Hare, C. E., Leblanc, K., Rose, J. M., Zhang, Y., DiTullio, G. R., et al. (2009). Effects of increased pCO2 and temperature on the North Atlantic spring bloom. I. The phytoplankton community and biogeochemical response. *Mar. Ecol. Prog. Ser.* 388, 13–25. doi: 10.3354/meps08133

Földer, S., Jaschinski, S., Wells, G., and Burns, C. W. (2010). Dominance and compensatory growth in phytoplankton communities under salinity stress. *J. Exp. Mar. Biol. Ecol.* 395, 223–231. doi: 10.1016/j.jembe.2010.09.006

Fujiwara, A., Hirawake, T., Suzuki, K., Imai, I., and Saitoh, S.-I. (2014). Timing of sea ice retreat can alter phytoplankton community structure in the western Arctic Ocean. *Biogeosciences* 11, 1705–1716. doi: 10.5194/bg-11-1705-2014

Fujiwara, A., Nishino, S., Matsuno, K., Onodera, J., Kawaguchi, Y., Hirawake, T., et al. (2018). Changes in phytoplankton community structure during wind-induced fall bloom on the Chukchi Shelf. *Polar Biol.* 41, 1279–1295. doi: 10.1007/s00300-018-2284-7

Gao, G., Jin, P., Liu, N., Li, F., Tong, S., Hutchins, D. A., et al. (2017). The acclimation process of phytoplankton biomass, carbon fixation and respiration to the combined effects of elevated temperature and pCO2 in the northern South China Sea. *Mar. Pollut. Bull.* 118, 213–220. doi: 10.1016/j.marpolbul.2017.02.063

Gao, K., Xu, J., Gao, G., Li, Y., Hutchins, D. A., Huang, B., et al. (2012). Rising CO2 and increased light exposure synergistically reduce marine primary productivity. *Nat. Clim. Change* 2, 519–523. doi: 10.1038/nclimate1507

Gattuso, J. P., Gao, K., Lee, K., Rost, B., and Schulz, K. (2011). "Approaches and tools to manipulate the carbonate chemistry," in *Guide to Best Practices for Ocean Acidification Research and Data Reporting*, eds U. Riebesell, V. J. Fabry, L. Hansson, and J. P. Gattuso (Luxembourg: Publications Office of the European Union), 41–52.

Grebmeier, J. M., Bluhm, B. A., Cooper, L. W., Danielson, S. L., Arrigo, K. R., Blanchard, A. L., et al. (2015). Ecosystem characteristics and processes facilitating persistent macrobenthic biomass hotspots and associated benthivory in the Pacific Arctic. *Prog. Oceanogr.* 136, 92–114. doi: 10.1016/j.pocean.2015.05.006

Harada, N. (2016). Potential catastrophic reduction of sea ice in the western Arctic Ocean: its impact on biogeochemical cycles and marine ecosystems. *Glob. Planet. Change* 135, 1–17. doi: 10.1016/j.gloplacha.2015.11.005

Hare, C. E., Leblanc, K., DiTullio, G. R., Kudela, R. M., Zhang, Y., Lee, P. A., et al. (2007). Consequences of increased temperature and CO2 for phytoplankton community structure in the Bering Sea. *Mar. Ecol. Prog. Ser.* 352, 9–16. doi: 10.3354/meps07182

Hasle, G. R., and Syvertsen, E. E. (1997). "Marine diatoms," in *Identifying Marine Phytoplankton*, ed. C. R. Tomas (London: Academic Press), 5–385. doi: 10.1016/b978-012693015-3/50005-x

Heiden, J. P., Völkner, C., Jones, E. M., van de Poll, W. H., Buma, A. G. J., Meredith, M. P., et al. (2019). Impact of ocean acidification and high solar radiation on productivity and species composition of a late summer phytoplankton community of the coastal Western Antarctic Peninsula. *Limnol. Oceanogr.* 64, 1716–1736. doi: 10.1002/lno.11147

Hillebrand, H., Durseien, C. D., Kirschtel, D., Pollingher, U., and Zohary, T. (1999). Biovolume calculation for pelagic and benthic microalgae. *J. Phycol.* 35, 403–424. doi: 10.1046/j.1529-8817.1999.3520403.x

Holding, J. M., Duarte, C. M., Sanz-Martín, M., Mesa, E., Arrieta, J. M., Chierici, M., et al. (2015). Temperature dependence of CO2-enhanced primary productivity in the European Arctic Ocean. *Nat. Clim. Change* 5, 1079–1082. doi: 10.1038/nclimate2768

Hoppe, C. J. M., Schuback, N., Semeniuk, D. M., Maldonado, M. T., and Rost, B. (2017). Functional redundancy facilitates resilience of subarctic phytoplankton assemblages toward ocean acidification and high irradiance. *Front. Mar. Sci.* 4:229. doi: 10.1007/s00300-017-2186-0

Hoppe, C. J. M., Flintrop, C. M., and Rost, B. (2018a). The Arctic picoeukaryote *Micromonas pusilla* benefits synergistically from warming and ocean acidification. *Biogeosciences* 15, 4353–4365. doi: 10.5194/bg-15-4353-2018

Hoppe, C. J. M., Schuback, N., Semeniuk, D., Giesbrecht, K., Mol, J., Thomas, H., et al. (2018b). Resistance of Arctic phytoplankton to ocean acidification and enhanced irradiance. *Polar Biol.* 41, 399–413. doi: 10.1007/s00300-017-2186-0

Hoppe, C. J. M., Wolf, K. K. E., Schuback, N., Tortell, P. D., and Rost, B. (2018c). Compensation of ocean acidification effects in Arctic phytoplankton assemblages. *Nat. Clim. Change* 8, 529–533. doi: 10.1038/s41558-018-0142-9

Hunt, G. L. Jr., Blanchard, A. L., Boveng, P., Dalpadado, P., Drinkwater, K. F., Eisner, L., et al. (2013). The Barents and Chukchi Seas: comparison of two Arctic shelf ecosystems. *J. Mar. Syst.* 10, 43–68. doi: 10.1016/j.jmarsys.2012.08.003

Hussherr, R., Levasseur, M., Lizotte, M., Tremblay, J. É, Mol, J., Thomas, H., et al. (2017). Impact of ocean acidification on Arctic phytoplankton blooms and dimethyl sulfide concentration under simulated ice-free and under-ice conditions. *Biogeosciences* 14, 2407–2427. doi: 10.5194/bg-14-2407-2017

Irigoien, X., Flynn, K. J., and Harris, R. P. (2005). Phytoplankton blooms: a 'loophole' in microzooplankton grazing impact? *J. Plankton Res.* 27, 313–321. doi: 10.1093/plankt/fbi011

Kawano, T., Aoyama, M., Joyce, T., Uchida, H., Takatsuki, Y., and Fukasawa, M. (2006). The latest batch-to-batch difference table of standard seawater and its application to the WOCE onetime sections. *J. Oceanogr.* 62, 777–792. doi: 10.1007/s10872-006-0097-8

Koenigk, T., Brodeau, L., Graversen, R. G., Karlsson, J., Svensson, G., Tjernstrom, M., et al. (2013). Arctic climate change in 21st centry CMIP5 simulations with EC-Earth. *Clim. Dyn.* 40, 2719–2743. doi: 10.1007/s00382-012-1505-y

Lalli, C. M., and Parsons, T. R. (1997). *Biological Oceanography. An introduction.* Oxford: Butterworth-Heinemann, 314.

Langer, G., Geisen, M., Baumann, K. H., Kläs, J., Riebesell, U., Thoms, S., et al. (2006). Species-specific responses of calcifying algae to changing seawater carbonate chemistry. *Geochem. Geophys. Geosystems* 7: Q09006. doi: 10.1029/2005/GC001227

Langer, G., Nehrke, G., Probert, I., Ly, J., and Ziveri, P. (2009). Strain-specific responses of *Emiliania huxleyi* to changing seawater carbonate chemistry. *Biogeosciences* 6, 2637–2646. doi: 10.5194/bg-6-2637-2009

Larsen, A., and Bryant, S. (1998). Growth rate and toxicity of *Prymnesium parvum* and *Prymnesium patelliferum* (haptophyte) in response to changes in salinity, light and temperature. *Sarsia* 85, 409–418. doi: 10.1080/00364827.1998.10413700

Lewis, E., and Wallance, D. W. R. (1998). *Program Developed for CO₂ System Calculations. ORNL/CDIAC-105. Carbon Dioxide Information Analysis Center.* Oak Ridge: Oak Ridge National Laboratory.

Li, G., and Campbell, D. A. (2013). Rising CO_2 interacts with growth light and growth rate to alter photosystem II photoactivation of the coastal diatom *Thalassiosira psudonana*. *PLoS One* 8:e55562. doi: 10.1371/journal.pone.0055562

Li, W. K. W., McLaughlin, F. A., Lovejoy, C., and Carmack, E. C. (2009). Smallest algae thrive as the Arctic Ocean freshens. *Science* 326:539. doi: 10.1126/science.1179798

Lovejoy, C., Vincent, W. F., Bonilla, S., Roy, S., Martineau, M. J., Terrado, R., et al. (2007). Distribution, phylogeny, and growth of cold-adapted picoprasinophytes in Arctic Seas. *J. Phycol.* 43, 78–89. doi: 10.1111/j.1529-8817.2006.00310.x

Marañón, E. (2015). Cell size as a key determinant of phytoplankton metabolism and community structure. *Annu. Rev. Mar. Sci.* 7, 241–264. doi: 10.1146/annurev-marine-010814-015955

Meakin, N. G., and Wyman, M. (2011). Rapid shifts in picoeukaryote community structure in response to ocean acidification. *ISME J.* 8, 1953–1961. doi: 10.1038/ismej.2011.18

Menden-Deuer, S., and Lessard, E. J. (2000). Carbon to volume relationships for dinoflagellates, diatoms, and other protist plankton. *Limnol. Oceanogr.* 45, 569–579. doi: 10.4319/lo.2000.45.3.0569

Nishino, S., Kawaguchi, Y., Inoue, J., Hirawake, T., Fujiwara, A., Futsuki, R., et al. (2015). Nutrient supply and biological response to wind-induced mixing, inertial motion, internal waves, and currents in the northern Chukchi Sea. *J. Geophys. Res.* 120, 1975–1992. doi: 10.1002/2014jc010407

Nishino, S., Kikuchi, T., Fujiwara, A., Hirawake, T., and Aoyama, M. (2016). Water mass characteristics and their temporal changes in a biological hotspot in the southern Chukchi Sea. *Biogeosciences* 13, 2563–2578. doi: 10.5194/bg-13-2563-2016

Overland, J. E., Wang, M., Walsh, J. E., and Stroeve, J. C. (2014). Future Arctic climate changes: adaptation and mitigation time scales. *Earth's Future* 2, 68–74. doi: 10.1002/2013ef000162

Proshutinsky, A., Dukhovskoy, D., Timmermans, M. L., Krishfield, R., and Bamber, J. L. (2015). Arctic circulation regimes. *Phil. Trans. R. Soc. A* 373:20140160. doi: 10.1098/rsta.2014.0160

Richier, S., Achterberg, E. P., Dumousseaud, C., Poulton, A. J., Suggett, D. J., Tyrrell, T., et al. (2014). Phytoplankton responses and associated carbon cycling during shipboard carbonate chemistry manipulation experiments conducted around Northwest European shelf seas. *Biogeosciences* 11, 4733–4752. doi: 10.5194/bg-11-4733-2014

Rose, J. M., and Caron, D. A. (2007). Does low temperature constrain the growth rates of heterotrophic protists? Evidence and implications for algal blooms in cold waters. *Limnol. Oceanogr.* 52, 886–895. doi: 10.4319/lo.2007.52.2.0886

Schaum, E., Rost, B., Millar, A. J., and Collins, S. (2013). Variation in plastic responses of a globally distributed picoplankton species to ocean acidification. *Nat. Clim. Change* 3, 298–302. doi: 10.1098/rspb.2014.1486

Schulz, K. G., Bach, L. T., Bellerby, R. G. J., Bermúdez, R., Büdenbender, J., Boxhammer, T., et al. (2017). Phytoplankton blooms at increasing levels of atmospheric carbon dioxide: experimental evidence for negative effects on Prymnesiophytes and positive on small picoeukaryotes. *Front. Mar. Sci.* 4:64. doi: 10.3389/fmars.2017.00064

Schulz, K. G., Bellerby, R. G. J., Brussaard, C. P. D., Büdenbender, J., Czerny, J., Engel, A., et al. (2013). Temporal biomass dynamics of an Arctic plankton bloom in response to increasing levels of atmospheric carbon dioxide. *Biogeosciences* 10, 161–180. doi: 10.5194/bg-10-161-2013

Serreze, M. A., and Barry, R. G. (2011). Processes and impacts of Arctic amplification: a research synthesis. *Glob. Planet. Change* 77, 85–96. doi: 10.1016/j.gloplacha.2011.03.004

Sugie, K., and Suzuki, K. (2015). Size of dominant diatom species can alter their evenness. *PLoS One* 10:e0131454. doi: 10.1371/journal.pone.0131454

Sugie, K., and Suzuki, K. (2017). Characterization of the synoptic-scale diversity, biogeography, and size distribution of diatoms in the North Pacific. *Limnol. Oceanogr.* 62, 884–897. doi: 10.1002/lno.10473

Sugie, K., and Yoshimura, T. (2013). Effects of pCO_2 and iron on the elemental composition and cell geometry of the marine diatom *Pseudo-nitzschia pseudodelicatissima*. *J. Phycol.* 49, 475–488. doi: 10.1111/jpy.12054

Sugie, K., and Yoshimura, T. (2016). Effects of high CO2 levels on the ecophysiology of the diatom *Thalassiosira weissflogii* differ depending on the iron nutritional status. *ICES J. Mar. Sci.* 73, 680–692. doi: 10.1093/icesjms/fsv259

Sugie, K., Yoshimura, T., and Wakita, M. (2018). Impact of CO2 on the elemental composition of the particulate and dissolved organic matter of marine diatoms emerged after nitrate depletion. *Limnol. Oceanogr.* 63, 1924–1943. doi: 10.1002/lno.10816

Suzuki, R., and Ishimaru, T. (1990). An improved method for the determination of phytoplankton chlorophyll using N. N-dimethylformamide. *J. Oceanogr. Soc. Jpn.* 46, 190–194. doi: 10.1007/bf02125580

Takishita, K., Nakano, K., and Uchida, A. (1999). Preliminary phylogenetic analysis of plastid-encoded genes from an anomalously pigmented dinoflagellate *Gymnodinium mikimotoi* (Gymnodiniales. Dinophyta). *Phycological Res.* 47, 257–262. doi: 10.1046/j.1440-1835.1999.00175.x

Thessen, A. E., Dortch, Q., Parsons, M. L., and Morrison, W. (2005). Effect of salinity on *Pseudo-nitzschia* species (Bacillariophyceae) growth and distribution. *J. Phycol.* 41, 21–29.

Thingstad, T. F., Øvreås, L., Egge, J. K., Løvdal, T., and Heldal, M. (2005). Use of non-limiting substrates to increase size; a generic strategy to simultaneously optimize uptake and minimize predation in pelagic osmotrophs? *Ecol. Lett.* 8, 675–682. doi: 10.1111/j.1461-0248.2005.00768.x

Thoisen, C., Riisgaard, K., Lundholm, N., Nielsen, T. G., and Hansen, P. J. (2015). Effect of acidification on an Arctic phytoplankton community from Disko Bay. West Greenland. *Mar. Ecol. Prog. Ser.* 520, 21–34. doi: 10.3354/meps11123

Tremblay, G., Belzile, C., Gosselin, M., Poulin, M., Roy, S., and Tremblay, J. E. (2009). Late summer phytoplankton distribution along a 3500 km transect in Canadian Arctic waters: strong numerical dominance by picoeukaryotes. *Aquat. Microbial. Ecol.* 54, 55–70. doi: 10.3354/ame01257

Trimborn, S., Thoms, S., Brenneis, T., Heiden, J. P., Beszteri, S., and Bischof, K. (2017). Two Southern Ocean diatoms are more sensitive to ocean acidification and changes in irradiance than the prymnesiophyte *Phaeocystis antarctica*. *Physiol. Plant.* 160, 155–170. doi: 10.1111/ppl.12539

Tuomisto, H. (2010). An updated consumer's guide to evenness and related indices. *Oikos* 121, 1203–1218. doi: 10.1111/j.1600-0706.2011.19897.x

Van Heukelem, L., and Thomas, C. S. (2001). Computer-assisted high-performance liquid chromatography method development with applications to the isolation and analysis of phytoplankton pigments. *J. Chromatgr.* 910, 31–49. doi: 10.1016/s0378-4347(00)00603-4

Watanabe, E., Onodera, J., Harada, N., Honda, M. C., Kimoto, K., Kikuchi, T., et al. (2014). Enhanced role of eddies in the Arctic marine biological pump. *Nat. Commun.* 5:3950. doi: 10.1038/ncomms4950

Welschmeyer, N. A. (1994). Fluorometric analysis of chlorophyll *a* in the present of chlorophyll *b* and pheopigments. *Limnol. Oceanogr.* 39, 1985–1992. doi: 10.4319/lo.1994.39.8.1985

Wolf, K. K. E., Hoppe, C. J. M., and Rost, B. (2018). Resilience by diversity: large intraspecific differences in climate change responses of an Arctic diatom. *Limnol. Oceanogr.* 63, 397–411. doi: 10.1002/lno.10639

Yamaguchi, M., Itakura, S., Nagasaki, K., Matsuyama, Y., Uchida, T., and Imai, I. (1997). Effects of temperature and salinity on the growth of the red tide flagellates *Heterocapsa circularisquama* (Dinophyceae) and *Chattonella verruculosa* (Raphidophyceae). *J. Plankton Res.* 19, 1167–1174. doi: 10.1093/plankt/19.8.1167

Yamamoto-Kawai, M., McLaughlin, F. A., Carmack, E. C., Nishino, S., Shimada, K., and Kurita, N. (2009). Surface freshening of the Canada Basin, 2003–2007: river runoff versus sea ice meltwater. *J. Geophys. Res.* 114:C00A05. doi: 10.1029/2008JC005000

Yamamoto-Kawai, M., Mifune, T., Kikuchi, T., and Nishino, S. (2016). Seasonal variation of $CaCO_3$ saturation state in bottom water of a biological hotspot in the Chukchi Sea. Arctic Ocean. *Biogeosciences* 13, 6155–6169. doi: 10.5194/bg-13-6155-2016

Yao, W., and Byrne, R. H. (1998). Simplified seawater alkalinity analysis: use of linear aray spectrometers. *Deep-Sea Res.* 45, 1383–1392. doi: 10.1016/s0967-0637(98)00018-1

Yasunaka, S., Siswant, E., Olsen, A., Hoppema, M., Watanabe, E., Fransson, A., et al. (2018). Arctic Ocean CO_2 uptake: an improved multiyear estimate of the air-sea CO_2 flux incorporating chlorophyll *a* concentrations. *Biogeosciences* 15, 1643–1661. doi: 10.5194/bg-15-1643-2018

Yoshimura, T., Sugie, K., Endo, H., Suzuki, K., Nishioka, J., and Ono, T. (2014). Organic matter production response to CO_2 increase in open subarctic plankton communities: comparison of six microcosm experiments under iron-limited and -enriched conditions. *Deep-Sea Res. I* 94, 1–14. doi: 10.1016/j.dsr.2014.08.004

Zapata, M., Fraga, S., Rodriguez, F., and Garrido, J. (2012). Pigment-based chloroplast types in dinoflagellates. *Mar. Ecol. Prog. Ser.* 465, 33–52. doi: 10.3354/meps09879